SEMMELWEIS EGYETEM

DOKTORI ISKOLA

Ph.D. értekezések

3053.

BOKHARI SYEDA MAHAK ZAHRA

Kórélettan és transzlációs medicina
című program

Programvezető: Dr. Benyó Zoltán, egyetemi tanár

Témavezető: Dr. Hamar Péter, egyetemi tanár

VASCULAR AND HYPOXIA DYNAMICS OF MURINE TRIPLE-NEGATIVE BREAST CANCER IN RESPONSE TO MODULATED ELECTRO-HYPERTHERMIA

PhD thesis

Syeda Mahak Zahra Bokhari

Semmelweis University Doctoral School,

Theoretical and Translational Medicine Division

Supervisor: Péter Hamar, DSc

Opponents: Éva Szőke, PhD
Dániel Sándor Veres, PhD

Head of the Complex Examination Committee: György Reusz, DSc

Members of the Complex Examination Committee: Tamás Radovits, PhD
Charaf Hassan, DSc

Budapest

2024

Contents

List of Abbreviations

AIF-1:	Apoptosis Inducing Factor-1
APC:	Antigen Presenting Cell
ASA:	Aspirin
BC:	Breast Cancer
BRCA:	Breast Cancer gene
BL-1:	Basal Like 1
BL-2:	Basal Like 2
cCa3:	Cleaved Caspase 3
COX-2:	Cyclo-oxygenase 2
DC:	Dendritic Cell
DDR:	DNA Damage Repair
DNA:	Deoxyribonucleic acid
dsDNA:	Double strand Deoxyribonucleic acid
ER:	Estrogen Receptor
FGF:	Fibroblast Growth Factor
TGF- β	Transforming Growth Factor β
PDGF:	Platelet Derived Growth Factor
VEGF:	Vascular Endothelial Growth Factor
HER-2:	Human Epidermal growth Factor Receptor 2
HIF1α:	Hypoxia Inducible Factor 1 α
HSP:	Heat Shock Protein
HT:	Hyperthermia
H2AFX:	H2A histone family member X

IDC:	Invasive Ductal Carcinoma
ILC:	Invasive Lobular Carcinoma
IM:	Immunomodulatory
LAR:	Luminal Androgen Receptor
LH:	Local Hyperthermia
M:	Mesenchymal
mEHT:	Modulated electrohyperthermia
MSL:	Mesenchymal stem like
NKs:	Natural Killer Cells
NFκB	Nuclear Factor Kappa B
NSAIDs:	Non Steroidal Anti Inflammatory Drugs.
PBS:	Phosphate Buffered Saline
PR:	Progesterone Receptor
RF:	Radiofrequency
RH:	Regional Hyperthermia
RNA:	Ribonucleic Acid
SAR:	Specific Absorption Rate
TNBC:	Triple Negative Breast Cancer
WBH:	Whole Body Hyperthermia

1. Introduction

1.1 Breast Cancer

Breast cancer (BC) is the most frequent cancer, affecting one in every eight women worldwide (120). Each year, the number of women diagnosed with breast cancer is increasing rapidly, and 16% of all the cancer-related deaths account for BC globally (18). Although non-malignant and local tumors are curable in 70-80% of patients, malignant breast cancer is a leading cause of cancer-related deaths worldwide with a less than 30% five-year survival rate (106).

1.1.2 Breast cancer histological subtypes

Breast cancer is usually of epithelial origin initiated either in the ductal or lobular region of the breast hence called ductal or lobular carcinoma (epithelial) (44). Most breast cancers are metastatic and are referred to as invasive ductal carcinoma (IDC), or invasive lobular carcinoma (ILC). About 80% of the BC cases are diagnosed when they are already systemic (invasive and thus, metastatic) (31). Their non-invasive counterparts, a localized carcinoma that has yet to break through the basal membrane, is called pre-invasive carcinoma or carcinoma in situ, namely ductal carcinoma in situ and lobular carcinoma in situ (44).

1.1.3 Breast cancer molecular subtypes

Besides the broad histological classification, BC subtypes have unique molecular subtypes (110) which mainly include a receptor-positive subtype with expressing Estrogen Receptor (ER) and/or Progesterone Receptor (PR) or Human Epidermal growth factor Receptor-2 (HER-2) (48). Perou and his colleagues classified BC based on comprehensive cDNA microarray profiling into four subtypes namely Luminal A, Luminal B, HER2+, and a receptor-negative subtype also called Triple-negative Breast Cancer (TNBC) (98). This pioneered the development of other mutagenic assays to characterize BC subtypes for effective treatment.

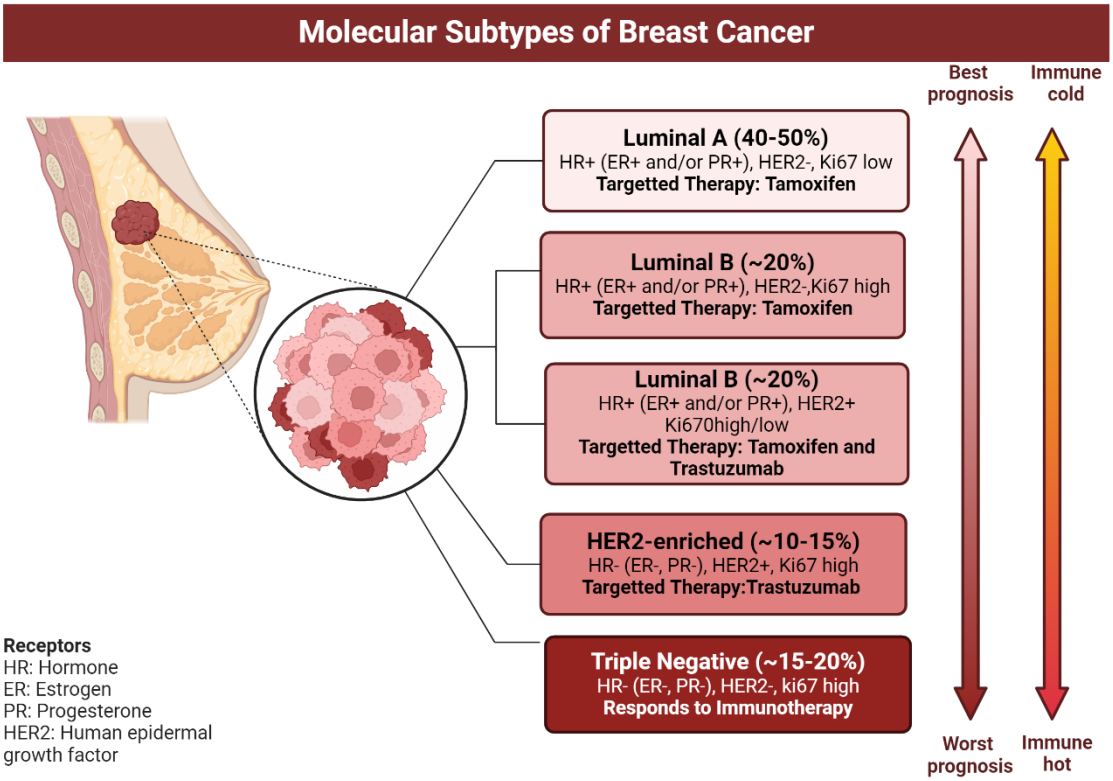

Figure 1: Molecular subtypes of Breast Cancer. Breast cancer classification based on molecular subtypes and their associated receptors. Each subtype has a unique immune and molecular profile with varying responses to therapy and variable prognosis (20, 35, 46). Created with Biorender.

1.1.4 Triple Negative Breast Cancer (TNBC)

Triple negative breast cancer is a highly aggressive breast cancer type lacking hormone receptors (ER and PR) and HER-2 receptor with poorly differentiated and heterogeneous biology. TNBC accounts for 15-20% of all BC cases detected with a high rate of relapse and the worst prognosis (163). Lehman and colleagues classified TNBC based on gene expression patterns into seven subtypes; Basal-like (BL) BL-1 & BL-2, Immunomodulatory (IM) subtype which expresses immune signalling genes, Mesenchymal (M) and Mesenchymal stem like (MSL) with high motility and expression of angiogenesis related genes, luminal androgen receptor (LAR) having androgen receptor activated gene expression and a complex unstable subtype (69). They further refined their classification to four main subclasses i.e. BL-1, BL-2, M and LAR as they

noticed the involvement of stromal and immune cells in the gene expression profile of MSL and IM subtypes (70).

Although BC is less immunoreactive than other immune-active cancer types, TNBC is the most immune-reactive among all subtypes due to the high expression of immune genes and a high intra-tumoral and stromal infiltration of lymphocytes (75). Different subtypes of TNBC have different immune profiles; the BL subtype is typically considered 'hot' compared to the LAR subtype with a 'cold' i.e. low tumor-infiltrating lymphocytes. The MSL subtype, however, is reported to have an immune-desert microenvironment (29). This classification by Lehman is generally accepted and considered in clinics to decide on suitable treatment options (161) however, TNBC demonstrates a high genetic and clonal diversity and heterogeneity within the same tumor and tumors from different patients (29, 116).

1.1.5. Treatment for breast cancer

Despite advances in medical therapy, the treatment of breast cancer is still challenging. In general, receptor-positive cancers have a better prognosis and can be treated with chemotherapy, endocrine therapy and HER-2 inhibitors (57). The main treatment goal for non-invasive BC is to remove tumors and prevent relapse, while in the case of metastatic cancer, the main goal is to manage metastasis and improve the patient's quality of life. The most common treatment options include surgery, radiotherapy, chemotherapy, bisphosphonates, HER-2 inhibitors and immunotherapy (57). However, each patient's treatment regimen is extensively tailored based on the cancer subtype and grade.

Triple negative breast cancer, however is the only BC subtype that lacks targeted treatment (163). Despite the immune reactivity in TNBC, immunotherapy agents only provide a modest benefit in combination with chemotherapy only when utilized as first-line treatment (113). Currently, TNBC therapy is reliant on devising an elaborate treatment plan including neo-adjuvant and adjuvant therapies and, in some cases, a dose dense scheduling i.e. increasing intensity of chemotherapy by either administering the drug more frequently or administration of a higher drug doses sequentially rather than a concurrent low dosage (40). Based on randomized clinical trials, incorporation of adjuvant therapy after neo-adjuvant immunotherapy and chemotherapy resulted in an 8%

and 5% increase in overall survival of TNBC patients respectively (81, 152). Similarly, dose dense scheduling of treatment is found to reduce the risk of recurrence in TNBC patients (40). Other major therapy options involve PARP inhibitors, antibody based drugs, immune checkpoint inhibitors and targeting of specific pathways (163). Despite recent developments in therapy types and treatment regimens, TNBC remains to be a challenging cancer type. The high heterogeneity, diverse pathophysiology and lack of specific targets calls for extensive research exploring better treatment options for TNBC. At present, adjuvant treatment options such as hyperthermia have a strong clinical indication in the case of TNBC.

1.1.6 Triple negative breast cancer mouse models; 4T1 and 4T07

Mouse models are an effective and economical tool to investigate mechanisms and pathways in vivo. Selection of an appropriate model based on research objectives is a crucial step for effective research. The most commonly used TNBC cell lines to create syngeneic models are 4T1 and 4T07, which are subclones of 410.4 mammary carcinoma cells, derived from a spontaneous breast cancer of the inbred Balb/c mouse (19). 4T1 is a highly tumorigenic and invasive cell type that has basal like characteristics (101). 4T1 tumors can spontaneously metastasize to other organs such as blood, brain, bone, lungs, liver and lymph nodes in a manner similar to human TNBC. Furthermore, the syngeneic model: the implantation of 4T1 cancer cells into Balb/c mice is genetically stable and transplantable making it an excellent model for translational research (97). Similarly, 4T1 cells can establish tumors in immunocompetent mice yet are poorly immunogenic, which mimics BC metastasis of humans(62, 73). 4T07 is another TNBC model cell line, subclone of the same 410.4 cell line which is highly tumorigenic but non metastatic. Although 4T07 cells can be found in lungs and blood, they fail to establish macro-metastasis at secondary sights. This inability is mainly attributed to a failure to extravasate the blood vessels. 4T07 is however immunogenic as compared to 4T1 which makes it a suitable model for immunotherapy research.

1.2 Hyperthermia in Oncology

Hyperthermia (HT) can be defined as the use of heat energy to target malignancy (124). De Kizowitz reported the reduction of tumor growth in patients suffering from malarial

fever in 1779, France. Effectiveness of hyperthermia as a cancer therapy has been under continuous scrutiny however, HT evolved to be a promising complementary therapy facilitating chemo-, radio- and other oncology therapies (89, 108). Clinical hyperthermia includes providing heat energy to the malignant cells raising their temperature to 40-43°C for a specified time. The elevated temperature is a marker of the heat energy absorbed by tumor cells initiating physiological, structural and chemical modifications in the tumor tissue. HT mediated cancer cytotoxicity is usually detected in the temperature range of 39-43°C, promoting chemotherapy delivery and tissue oxygenation at about 40°C, impeding microcirculation at >41°C and cell death at 42°C (27).

HT directly damages the cancer cells by damaging chromosomes in S-Phase and disrupting the mitotic apparatus during the M-phase of the cell cycle (154). Furthermore, HT promotes cancer cell death by inducing structural and conformational changes in macro-molecular structures, disruption of cell metabolism, inhibition of DNA damage repair (DDR) mechanisms and activation of the cell's apoptotic pathways (13, 47, 108). Clinical evidence potentiated the benefits of hyperthermia in combination with radio- and chemo- therapy (93). It was reported that since radiotherapy mediates cytotoxicity by inducing DNA damage and generation of double strand breaks, HT promotes radiotherapy damage by inhibiting DDR either by altering the nuclear protein content (107) or damaging enzymes involved in DDR (47, 50). Similarly, the elevated temperature promotes vasodilation (26) facilitating enhanced blood flow, hence promoting chemotherapy delivery to the tumor core, (47, 93). Simultaneously, HT increases cell membrane fluidity thereby altering the cell membrane potential that leads to enhanced drug uptake by the cancer cell (93, 115, 141).

1.3 Modulated electro-hyperthermia

Modulated electro-hyperthermia (mEHT) also termed as oncothermia, is a non-invasive loco-regional hyperthermia based treatment modality which uses radiofrequency (RF) current at 13.65 MHz to selectively heat cancer cells (125). Modulated radiofrequency current flows through the patient's tumor region sandwiched between two cooling condenser electrodes. The energy generated is absorbed specifically by the cancer cells leading to an increase in temperature of the tumor (124). Notably, mEHT establishes a

2.5°C temperature difference between the tumor core and the skin temperature above the tumor (28). mEHT can selectively target cancer cells while exempting healthy cells due to the following altered biophysical and metabolic properties of cancer cells.

- Cancer cells tend to rely on anaerobic glycolysis regardless of the presence of oxygen (Warburg effect) which on one hand reduces the extracellular pH due to lactic acid production and on the other hand increases electrical conductance hereby allowing better selection of the cancer tissue by mEHT (131).
- Cancerous and healthy cells differ in their dielectric properties: cancer cells have higher dielectric permittivity and lower membrane potential. Furthermore, the low amount of ATP produced by cancer cells is not sufficient to regulate active membrane potential which adds to a reduced membrane potential of cancer cells (15, 129).
- Physiological differences such as the altered lipid and sterol composition and higher numbers of membrane rafts (transmembrane domains enriched with sterols and spingolipids) in the cancer cell's membrane as compared to healthy cells further facilitates the selection of cancer cells by mEHT (124, 129).

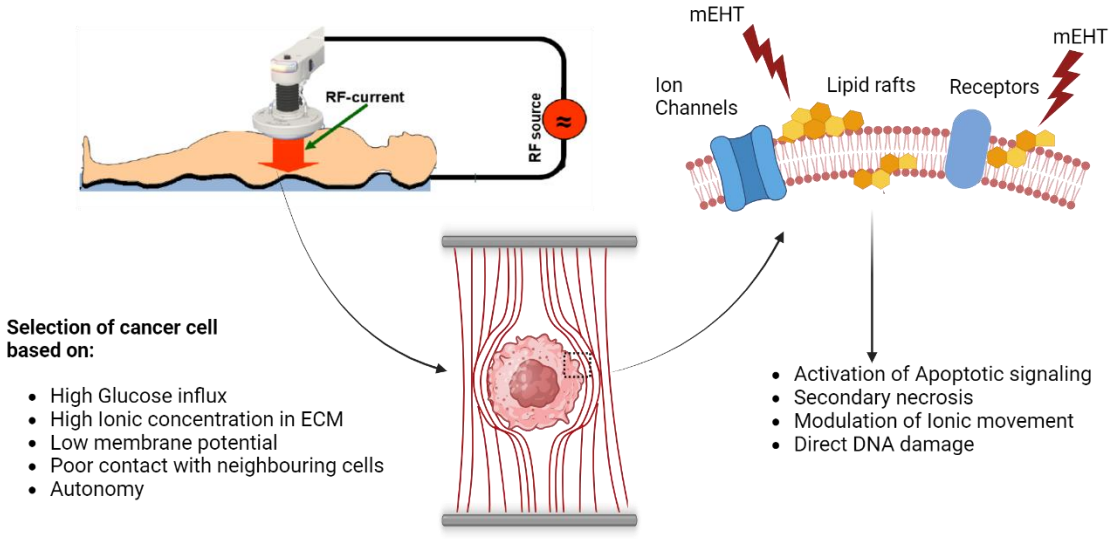

Figure 2: Principle of modulated electrohyperthermia treatment. Tumor is placed between two electrodes and a radiofrequency current runs through the circuit of which the patient is a part. The radiofrequency current generates an electromagnetic field which is specifically absorbed by cancer cells due to their altered physiological and metabolic

properties. The energy is absorbed by lipid rafts of the cancer cell's membrane thereby activating nearby signalling receptors and altering ion movement across the membrane which collectively contributes to cancer cell death selectively (17, 84, 123). Created with Biorender.

Modulated electro-hyperthermia provides local heating by specifically heating membrane rafts and extracellular electrolytes of the extracellular environment thereby heating up only a narrow and specific region of the cancer cell's plasma membrane which prevents formation of hotspots like in whole body hyperthermia. (15). Principally, the heat energy is absorbed by the extracellular electrolytes which heat up and create a temperature difference between the extracellular and intracellular environment of the cancer cell. This heterogeneity firstly facilitates continuous heat flow across the selected cells and secondly promotes apoptotic signalling (124). Membrane rafts have high conductivity and permeability which allows better current flow and hence absorb maximum heat energy thereby acting as nanofocus points i.e. biological nanoparticles, for mEHT (42, 96). Since membrane rafts have signalling proteins in close proximity, an altered physiology of the membrane rafts in response to energy absorption activates FAS signalling and hence caspase dependant apoptosis, mitochondrial apoptosis signalling and other signalling pathways (61). The radiofrequency current is better absorbed by the membrane rafts which not only activates apoptotic signalling but also creates a direct current voltage of approximately 1uV (156). This voltage difference creates ion efflux and hence upsets the ionic equilibrium of most ions across the cell membrane. This disruption of ionic equilibrium leads to cytotoxic effects for example, a severe K^+ ion efflux depolarizes the membrane and induces apoptosis, increased influx of Na^+ and Cl^- ions lead to cell swelling and trigger cell death. Similarly, an influx of Ca^+ ions potentiate apoptotic cell death. Overall, the disequilibrium of ions across the membrane reduces proliferation and clonogenicity of cancer cells (53, 128, 156). The most well-known, non-thermal, cytotoxic effect of an electromagnetic field is electroporation: pore formation on the cell membrane in an electromagnetic field.

1.3.1 Dosage, Heat and Temperature

It is of absolute importance to mention that though often used in the same context, absorbed heat energy and not the temperature is the driver of mEHT (84). In case of

mEHT, energy is the key player while elevated temperature is a mere response to energy absorption (65). To define a dosage, we need to define an expected effect which in oncological hyperthermia is the damage of cancer tissue. It is however not very simple to define the dosage i.e. the maximal tolerable or minimal effective application of mEHT to obtain cytotoxic effects, as the energy absorbed and the energy dissipated in the cancer cell is highly heterogenous (123, 148). The absorption of heat is dependent on various factors which include the mass or volume of the target tissue and its bioelectric properties, for instance cancer cells have higher dielectric constants as compared to healthy cells but tumors with high fat content have lower dielectric constants. The dielectric properties of a tumor type may also vary depending on the stage of the cancer (100). Furthermore, the energy absorption and distribution to the target tissue are not the same as some of the energy is lost at the surface, some is dissipated from the target tissue to the surrounding tissue due to continuous blood flow and other is lost to the surface cooling mechanisms (130). The efficiency of energy absorption can therefore vary based on the given conditions of treatment, the actual target organ, frequency of the current and the frequency of the treatment events. In general, dose for mEHT is calculated as the energy absorber per unit of the tumor mass i.e. J/Kg, following the same principle of defining dose of ionizing radiations. The dose is defined as Specific Absorption Rate (SAR) in W/kg which depends on the maximum power provided by the mEHT device. Dose per session is calculated as the SAR times duration of active mEHT treatment. The treatment dose is the sum of all SARs in each session of treatment (84). Interestingly, in mEHT treated pork meat, scientists could observe a 92% energy absorption efficiency (92) and the combined thermal and non-thermal effects of mEHT could induce a three times higher cell distortion in comparison to sole thermal effects of conventional HT (148). Apart from the efficiency of energy absorption, the power applied and the intra-tumoral temperature achieved is also important. A high-power dosage at 18W during initial phases of mEHT i.e. elevation of temperature from 25°C to 37°C and from 37°C to 42°C provided higher apoptosis rate in the cancer cells as compared to lower power i.e. 7.6W applied while maintaining the temperature at 42°C. Hence, a large dose of power and accumulation of power over a longer duration yielded the best cytotoxic effects (56). It is therefore necessary to determine the optimal dosage in clinical settings based on frequent evaluations and feedback to ensure effective anticancer treatment.

1.3.2 Biological effects of modulated electro-hyperthermia

Modulated electrohyperthermia induces various cellular responses owing to its synergistic thermal and non-thermal effects. The most prominent cytotoxic biological effect of mEHT is activation of programmed cell death in cancer cells. mEHT can initiate apoptotic signalling, nuclear shrinkage, membrane blebbing and formation of apoptotic bodies (61). mEHT induces apoptosis dependant or independent cleaved caspase 3. In vitro studies showed an increase in pro-apoptotic and reduction of anti-apoptotic factors after a single treatment with mEHT in the colorectal cancer cell line C26. This apoptosis initiation led to a significant cleaved caspase 3 (cCa3) mediated apoptosis after 24 hours (142). Similar effects were observed in the HepG2, hepatocellular carcinoma cell line after three mEHT treatments (159). mEHT mediated cCa3 dependant apoptosis was also confirmed in a TNBC mouse model (28). Besides the caspase mediated apoptosis, mEHT can induce programmed cell death via other pathways such as upregulation of FAS and JNK signalling pathways (17). Furthermore, mEHT upregulates expression of Apoptosis inducing factor 1 (AIF-1) and facilitates its release from the mitochondrial membrane thereby translocating to the nucleus and promoting DNA fragmentation (21)

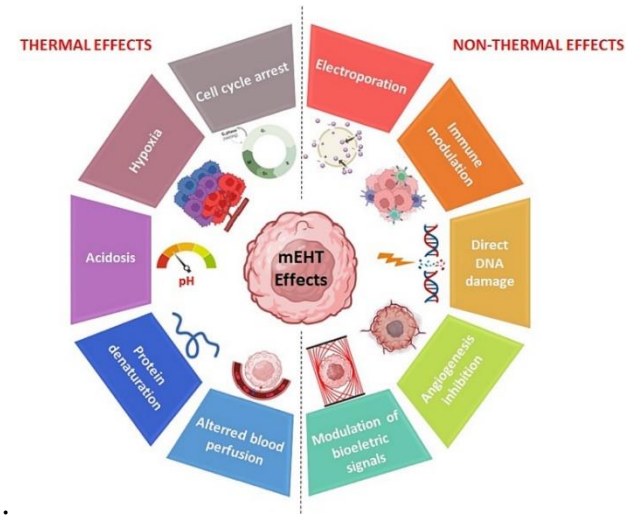

.

Figure 3: Biological effects of modulated electrohyperthermia. Cancer cells specifically absorb electromagnetic energy across the several membrane rafts of the cell membrane and the tumor is heated up. The thermal and non-thermal effects of modulated electrohyperthermia synergistically interfere with the cell's physiology and lead to apoptosis (61, 84, 147). Created with Biorender.

mEHT further induces double stranded DNA (dsDNA) breaks in colorectal cancer C26 and melanoma B16F10 cells (82, 143) which could be detected by strong phosphorylation of histone molecules, a marker of dsDNA damage translated to an enhanced expression of H2A histone family member X (γH2AX) (36). This high expression of γH2AX promotes cell damage by reducing BReast CAncer gene (BRCA-2) expression thereby halting DNA repair and promoting release and nuclear translocation of Apoptosis Inducing factor-1 (AIF-1) (21), promoting apoptosis. γH2AX also promoted expression of p21 which halts cell cycle progression (37), this upregulation was also observed in colorectal cancer C26 (143) hepatocellular carcinoma HepG2 (54) and glioma cell line (B16F10) and glioma xenograft models (82).

Cancer cells respond to mEHT by eliciting stress responses such as upregulation of heat shock proteins (HSPs) in response to high thermal energy absorption. HSPs are chaperones that support conformation of proteins and macromolecules to prevent aggregation and or denaturation (117). mEHT induced expression of several HSPs namely HSP40, HSP60, HSP70 and HSP90 four hours after treatment which doubled after 24h in HT29 cells (16). Similarly, in our experiments, in TNBC isografts, HSP70 expression peaked at 12 hours followed by exhaustion at 24hours after three mEHT treatments (28).

Blood flow plays an interesting role in hyperthermia. In conventional whole body hyperthermia, temperature of the body rises and heats up the blood, this heated blood then reaches the tumor tissue and heats up the cancer cells. In local hyperthermia however, heat is applied directly to the tumor area and flowing blood acts as a cooling agent and dissipates the heat that reaches the tumor (41). During mEHT, the tumor is locally heated and hence blood flow dissipates heat, however when the temperature between the tumor core and the external environment gains equilibrium the specific energy of the electromagnetic field spreads to the points of equilibrium and reinstates lost heat, hence temperature is not reduced in response to blood flow as SAR replenishes energy to the tumor tissue (84).

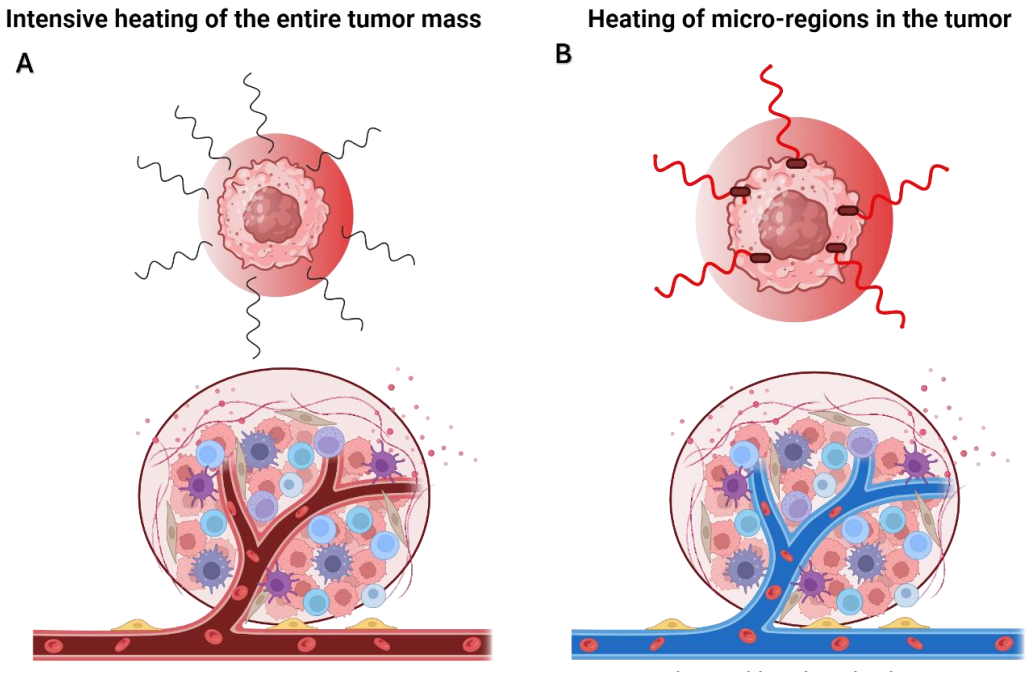

Figure 4: Role of blood flow in hyperthermia. (A) In whole body hyperthermia, the body temperature is elevated by fever or fever like stimuli which leads to heating up the blood. The heated blood circulates in the body and upon reaching the tumor mass heats up the tumor thus, the heating is not tumor selective. **(B)** In modulated electrohyperthermia, the tumor is directly heated by absorption of electromagnetic energy by lipid rafts of the cell membrane acting as biological nanoparticles and the flowing blood acts as a cooling agent maintaining a slight yet continuous temperature difference between the cancer mass and its surroundings (84, 123). Created with Biorender.

However as blood flow significantly modifies the SAR, temperature detection in the tumor is not the most accurate way to determine mEHT dosing (84, 129). Mild hyperthermia promotes blood flow by vasodilation which on one hand promotes tumor oxygenation and drug delivery while on the other hand promotes nutrient delivery and dissemination of cancer cells to secondary sites.

Modulated electrohyperthermia therefore targets cancer cells by synergistic thermal and non-thermal effects which includes direct DNA damage, activation of apoptotic signalling, cellular stress and immune responses etc (147).

1.4 Cancer angiogenesis and hypoxia

A cancerous cell's ability to induce angiogenesis is one of the hallmarks of cancer, as angiogenesis is essential for tumor cells to survive (121). Unlike normal blood vessels, blood vessels in tumors are more permeable and tortuous, which is attributed to the altered endothelial cells (ECs) referred to as Tumor Endothelial Cells (TECs) (79, 132). Furthermore, besides the autocrine production of proangiogenic factors by tumor cells, tumor cells can prime immune cells to produce more angiogenic factors, which results in a loss of balance between the pro- and antiangiogenic factors, rendering the tumor vasculature unruly and poorly developed (94). Tumour blood vessels thereby have loose junctions, an incomplete basement membrane distribution, and reduced pericyte support. This deformed vascular physiology leads to poor blood supply and, therefore, hypoxia and reduced drug delivery (78, 169). The abnormal morphology of the tumor vasculature hinders blood perfusion and hence reduces the oxygen supply in the tumor core, promoting a hypoxic tumor microenvironment (160). This hypoxic microenvironment promotes angiogenesis to ensure survival and proliferation of the cancer (111). Tumor angiogenesis is initiated in response to hypoxic or inflammatory stimuli in the tumor microenvironment. During the angiogenic switch, ECs are activated and start to produce angiogenic growth factors such as Fibroblast Growth Factors (FGFs), Transforming Growth Factor β (TGF-β), Platelet Derived Growth Factor (PDGF), and Vascular Endothelial Growth Factors (VEGFs) (14, 169). The tumor vasculature is an important and complex factor in the cancer cell's survival and proliferation. Although inhibition of angiogenic pathways has provided better patient outcomes in clinical settings, resistance to antiangiogenic therapy (104) and tumor cells switching to other neovascularization processes are prominent challenges (105).

1.5 mEHT: a potentiator of repurposed anticancer drugs

Modulated electrohyperthermia is a prominent complementary treatment employed with chemo- and radiotherapy. Combining mEHT with radiotherapy provided better tumor regression and reduced gastrointestinal toxicity in locally advanced rectal cancer patients (58). Similarly, mEHT provided better overall treatment response in combination with platinum based chemotherapy in cervical cancer patients as compared to patients receiving only chemotherapy (68). mEHT also potentiated the effects of doxorubicin in

activating apoptosis and cell cycle arrest in murine colorectal cancer model (142). Furthermore, mEHT enhanced antitumor efficacy of intra-tumoral dendritic cell therapy in squamous cell carcinoma murine model by its abscopal effect (102). In a randomized clinical trial, mEHT was combined with common analgesic Nefopam. The study indicated that mEHT can enhance the bioavailability of orally consumed nefopam without increasing side effects (66). Hence it is practical to combine mEHT with available drugs to test if and how modulated electrohyperthermia enhances the drugs effectivity.

Similarly, repurposing already approved drugs for their acticancer potential has recently gained attention of the scientific community because it can reduce the cost and time required to identify and test new drugs for their efficacy and safety (157). Several classes of drugs are being tested to utilise their off target effects against several mechanisms of tumor progression (139). It would therefore be interesting if mEHT can potentiate the efficacy of such repurposed drugs to reduce overall treatment time .

1.6 Digoxin: cardiac glycoside with anticancer abilities

Digoxin, a cardiac glycoside, is a Na/K ATPase inhibitor (83) and a common drug of choice for patients with arrhythmias and congestive heart failure. Over the years, its potential as an anticancer therapy has been investigated (119, 166, 170) either alone or in combination with chemotherapeutics (151). It has now been established that dioxin and other cardiac glycosides provide anticancer effects by inhibiting proliferation and metastasis (51, 103). The effectiveness of digoxin in combination with chemotherapies such as doxorubicin (168), adriamycin (153), and gemcitabine (170) have been already investigated.

Digoxin's anti-cancer abilities could be attributed to its ability to inhibit the membrane Na^+/K^+ ATPase leading to alterations in intracellular Na^+ and Ca^+ concentrations thereby inducing apoptosis, autophagy, and immunological cell death (153). Furthermore, digoxin reduces expression of nuclear factor erythroid 2– related factor 2 (NRF-2) via downregulation of PI3K/Akt signalling which promotes oxidative damage to cancer cells (27). Zhang et al. reported that digoxin potently inhibited HIF1-α translation and reduced tumor volume (166). Similarly, digoxin inhibited HIF1- α transcription in mice reversing hypoxic pulmonary hypertension (12). Digoxin has demonstrated reproducible inhibition

of growth, invasion and epithelial to mesenchymal transition in cancer cell lines by downregulating HIF1-α expression (55, 77). It also reduced expression of genes in response to chemotherapy in BC by inhibiting the accumulation of HIF1-α (76). Furthermore, digoxin could reduce expression of Vascular Endothelial Growth Factor (VEGF) and N-myc downstream regulated gene 1 (NDRG1) in lung adenocarcinoma cells via HIF1-α inhibition (32). Ability of digoxin to reduce tumor proliferation and angiogenesis has been reported in various cancer types (122, 138, 153). There are several clinical trials running to assess the ability of digoxin as a treatment modality for cancer (1, 3-11).

1.7 Non-Steroidal Anti-inflammatory drugs as anticancer treatments

Non steroidal anti inflammatory drugs (NSAIDs) have also provided anticancer effects in several cancers. Chronic inflammation is a hallmark of cancer and cyclo-oxygenase 2 (COX-2) is a key player in modulating cancer therapy by production of prostaglandins, which promote inflammation, proliferation, survival, promoting angiogenesis and allowing immune suppression. It has therefore been implicated in the progression of various cancers including breast, lung, and prostate cancer (45, 72). NSAIDs express anti-tumor afctivity primarily by inhibiting activity of cyclo-oxygenase enzyme that leads to synthesis of prostaglandins (133). Knockout preclinical studies demonstrated that silencing COX-2 could reverse immunosuppression in murine melanoma model (165). Cox-2 inhibition by selective or non-selective inhibitors also translates to alleviation of inflammatory tumor environment (167).

Aspirin (ASA) has been thoroughly investigated for its anticancer effects and has shown promising effects in colorectal cancer patients. Aspirin can provide anticancer effects not only by targeting COX-2 but also by inhibition of Nuclear Factor Kappa B NFκB and polyamide catabolism (71, 136). ASAs potential as an anticancer drug is being investigated in several cancer types such as breast cancer, gastric cancer, pancreatic cancer, etc (52). Similarly, Inhibition of COX-2 by selective inhibitor Celecoxib reduced growth and metastasis in colorectal cancer in mice (23). COX-2 inhibition prevents cancer progression and migration in various cancers and promotes treatment efficacy of chemotherapy and radiotherapy (45, 109).

Pre-clinical mEHT studies demonstrate induction of damage associated proteins and pro-inflammatory cytokines in melanoma and BC models (61, 144) and as mEHT reduces hypoxia mediated gene expression (61) we hypothesized, that combining these repurposed drugs with modulated electrohyperthermia might have synergistic effects.

1.8 Clinical applications of modulated electro-hyperthermia

Modulated electrohyperthermia has been applied for almost twenty years currently being used in 32-34 countries (15). In clinical settings, mEHT has demonstrated significant improvement in patients with breast, pancreatic, ovarian, cervical, brain and gastrointestinal cancer (64, 85, 127). mEHT can be safely employed in clinics without significant side effects as observed in Phase I clinical trial of glioblastoma patients treated with mEHT in combination with chemotherapy. Similarly, mEHT could be safely combined with radiotherapy in grade III and IV glioblastoma patients (126, 155). Patients with inoperable and/or grade III and IV pancreatic cancer treated with mEHT had a better response, stabler disease and better overall survival as compared to control group both in combination with chemo or radiotherapy and as monotherapy (33, 34, 99).

mEHT also demonstrated feasible results in cervical cancer patients (162) with a significant improvement in disease free survival and quality of life (88) and overall survival (68). Another phase III clinical trial demonstrated the ability of mEHT to potentiate abscopal effects in combination with chemoradiotherapy (CRT) as compared to patients only receiving CRT in locally advanced cervical cancer patients (86, 87).

Similarly, combination of mEHT with traditional Chinese medicine provided better disease management with less toxicity in peritoneal carcinoma (95). In advanced rectal cancer, mEHT improved cancer regression and could provide better effects at lower dosage of radiotherapy with less toxicity and better disease free survival (58). A small clinical study also reported better quality of life in advanced metastatic BC patients when other treatment options were not working well (91). A new clinical trial assessing the benefits of applying mEHT in combination with neo-adjuvant chemotherapy namely paclitaxel, doxorubicin and carboplatin in HER2- breast cancer patients is currently recruiting (2).

2. Objectives

Studies described in the present dissertation are aimed at investigating the molecular mechanisms and pathways of repair initiated in triple negative breast cancer in response to modulated electrohyperthermia.

1. To investigate the effect of repeated modulated electrohyperthermia on the vasculature of TNBC tumors.
2. The time kinetic assessment of vascular and hypoxic dynamics.
3. To investigate the role of mEHT in initiating angiogenesis.
4. Inhibition of mEHT induced hypoxia and angiogenic repair by repurposing digoxin as an inhibitor if HIF1-α transcription.
5. To investigate the effect of mEHT therapies combined with either digoxin or SC-236.

3. Methods

3.1 Cell culture

4T07 and 4T1 cells were grown as adherent culture in Dulbecco's Modified Essential Medium (DMEM 4.5 g/L glucose with L-glutamine, #12-604F, Lonza A. G., Basel, Switzerland) supplemented with 10% Fetal Bovine Serum (FBS Catologue#ECS0180L, Euroclone S.p.A., Pero, Italy), and 10% Penicillin-Streptomycin (#17-602E, Lonza A. G., Basel, Switzerland).

3.2 In-vivo model

Six-to-eight-week-old female BALB/c mice were raised in the SPF animal facility of the Department of Oncology, Semmelweis University with ad libitum access to standard rodent chow and water, under 12 h dark/12 h light cycles. Animals were anesthetized for tumor cell-inoculation with isoflurane (Baxter International Inc., Deerfield, IL, USA) in 4–5% concentration for induction and 1.5–2% to maintain anaesthesia with 0.4–0.6 l/min compressed airflow. 1×10^6 4T1 cells in 50ul Phosphate Buffered Saline ((PBS) without Calcium and Magnesium #17-516F, Lonza A.G., Basel, Switzerland) solution were subcutaneously inoculated by 50µL Hamilton syringe (Hamilton Company, Reno, NV, USA). Inoculation was made orthotopically into the 4th mammary gland's fat pad in each mouse. Eight days after inoculation, tumors were measured with digital calliper and ultrasound and mice were randomized into mEHT and sham-treated groups according to tumor size and body weight. Mice were injected daily with 2mg/kg dose of digoxin (Merck Life Science Kft. D6003), SC236 6 mg/kg (Axon Medchem BV, Groningen, The Netherlands) or saline for eight days. Twenty-four hours after the last treatment mice were euthanized by cervical dislocation under anaesthesia. The tumors were resected and cleaned of the surrounding connective tissue, fat, and skin. The condition of the internal organs (bowels, urinary bladder, spleen) and possible adherences between the tumor and muscles were inspected. Tumors were cut in half along their longest diameter, one half was placed in a 4% buffered formaldehyde solution (Molar Chemicals Kft., Halásztelek, Hungary). The other half of the tumors were frozen in liquid nitrogen for molecular analysis (RNA isolation, RT-PCR). For time kinetics experiments, mice were euthanized, and tumors were harvested at different time points: 4, 12, 24, 48, and 72 h after the last treatment, and mice were injected with pimonidazole hydrochloride (HypoxyprobeTM1,

HPI catalogue no. HP1-200) by tail vain injection an hour before tumor harvest. Interventions and housing of the animals conform to the Hungarian Laws No. XXVIII/1998 and LXVII/2002 about the protection and welfare of animals, and the directives of the European Union. Animal experimental protocol was approved by the National Scientific Ethical Committee on Animal Experimentation under Nos. PE/EA/633-5/2018 and PE/EA/50-2/2019.

3.3 In-vivo mEHT treatments

Tumors were treated 3–5 times with the newly developed rodent modulated electro hyperthermia device as described previously (28, 114). The principle of the treatment is a capacitive coupled, amplitude-modulated, 13.56 MHz electromagnetic field which transfers energy to the tumors. Animals were placed on a heating pad (in vivo applicator), functioning as the lower electrode, and connected to the LabEHY modulated electro hyperthermia 200 device with heating and radiofrequency (RF) cable. The abdominal area below the mobile electrode and the back of the mice was shaved before the treatments to enable electric coupling. Treatments were performed with a LabEHY 200 device in a temperature-driven way, for 30 min with 0.7 ± 0.3 watts after a 5-min-long warmup. Temperature monitoring was performed with optical temperature sensor Luxtron (Oncotherm Ltd., Budaörs, Hungary). Temperature parameters were set and monitored as per our previously demonstrated guidelines (28). During sham treatments, the electromagnetic field was turned off, but all other conditions (heat pad temperature, upper electrode position) were similar to the mEHT treatment.

3.4 Matrigel plug assay and flow cytometry

To visualize and analyse the effect of mEHT on vascularization in vivo we performed a Matrigel plug assay. Eight to ten-week-old male C57BL/6 mice were raised in the Department of the Animal Facility of the Basic Medical Science Center of Semmelweis University. 500µL liquid Matrigel (BD Biosciences) containing 600 ng/ml bFGF were injected subcutaneously into the left and right groin regions of mice. On day 3 the right-side plugs were treated with mEHT and the left-side plugs were used as controls. The treatment was repeated twice every other day. After 8 days the plugs were excised and

subjected to measure the haemoglobin content by hemoglobin Assay Kit (Sigma-Aldrich,) or to flow cytometry.

Matrigel plugs were treated with Liberase TM (Roche Diagnostics) at 37 C for 30 min. The digested plugs were then filtered through a 70-um cell strainer and red blood cells were eliminated by Red Blood Cell Lysis buffer (BioLegend; San Diego, CA, USA), centrifuged for 5min at 350xg, washed with PBS, and fixed and permeabilized with Intracellular Fixation & Permeabilization Set (eBioscience). TruStain FcX antibody (Biolegend; San Diego, CA, USA) was used for blocking the non-specific binding of IgG to the Fc receptors. Immunostaining was performed by incubating the cells with monoclonal antibodies for 30 min on ice. The following antibodies were used: PE anti-mouse CD31 Antibody and APC anti-mouse CD45 Antibody (Biolegend) San Diego, CA, USA). Flow cytometry was performed with a FACS Calibur (Becton Dickinson, Mountain View, CA, USA). Frequency and intensity measurements were calculated in CellQuest software (Beckton Dickinson).

Table 1. Antibodies used for Flow cytometry.

Antibody	Type	Catalogue no.	Vendor
APC CD-45	Mouse, mAb	103111	Biolegend
CD-31	Mouse, mAb	102407	Biolegend

3.5 qPCR

RNA isolation was performed with TRI reagent (Molecular Research Center lnc., Ohio, USA) according to the manufacturer's instructions. Isolated RNA was reverse transcribed by High-Capacity cDNA Reverse Transcription Kit (Applied Biosystems, Carlsbadm, CA, USA). The amplified cDNA was used as a template for RT-PCR. Messenger RNAs were detected in the samples by SYBR Green based RT-PCR with SsoAdvanced™ Universal SYBER® Green Supermix and the CFX96 Touch Real-Time PCR Detection

System (Bio Rad, Hercules, CA, USA). Expressions were normalized to 18S. The used primers are listed in Table 3.

Table 2. Primers used for RT-PCR.

Gene symbol	Gene name	Primer pairs
18S	18S [Mus musculus]	Fwd: CTCAACACGGGAAACCTCAC Rev: CGCTCCACCAACTAAGAACG
CD105	Endoglin [Mus musculus]	Fwd: TGGATACCGGATAAGGCCCA Rev: CCGACTCTTTCTGCGAGACC

3.6 Histology and Immunohistochemistry

Formalin-fixed tumor samples were dehydrated and embedded in paraffin. Serial sections (2.5 μm) were cut and mounted on salinized glass slides, and kept in a thermostat at 65 °C for 1 h. Sections were dewaxed and rehydrated for haematoxylin-eosin (H&E) staining and immunohistochemistry (IHC). Endogenous peroxidases were blocked for 15 min using 3% H2O2 in methanol. For antigen retrieval, slides were subjected to constant heating for 20 min in (Tris-EDTA (TE) buffer pH 9.0 (0.1 M Tris base and 0.01 M EDTA) or (citrate buffer pH 6.0 (Dako, Glostrup, Denmark)) for CD-31 and anti-pimonidazole staining respectively, using an Avair electric pressure cooker (ELLA 6 LUX(D6K2A), Bitalon Kft, Pécs, Hungary). Followed by a 20-min cooling with an open lid. The non-specific proteins were blocked by incubation with 3% bovine serum albumin (BSA, #82-100-6, Millipore, Kankakee, Illinois, USA) diluted in 0.1 M Tris-buffered saline (TBS, pH7.4) containing 0.01% sodium azide for 20 mins. The sections were incubated with the primary antibodies diluted in 1% BSA/TBS + TWEEN (TBST, pH 7.4) (Table 1.) overnight in a humidity chamber. Peroxidase-conjugated anti-rabbit & anti-mouse IgGs (HISTOLS-MR-T, micropolymer -30011.500T, Histopathology Ltd., Pécs, Hungary)

were used for 40 min incubations and the enzyme activity was revealed in 3, 3'-diaminobenzidine (DAB) chromogen/hydrogen peroxide kit (DAB Quanto-TA-060-QHDX-Thermo Fischer Scientific, Waltham, MA, USA) under microscopic control. All incubations were at room temperature with the samples washed between incubations in TBST buffer for 3 × 3 min. Digital evaluation of Tumor Destruction Ratio (TDR%) on H&E slides and the CD31 and pimonidazole staining was performed using the case viewer software as described earlier (28). Red blood cell covered area was quantified by the CaseViewer software by double masking the whole tumor area (Parameters attached in supplementary data). Number of viable blood capillaries per tumor area was manually counted, viable vessels were characterised as circular, luminal, surrounded by living cells, visibly containing RBCs with area no less than $100um^2$.

Table 3. Antibodies used for Immunohistochemistry.

Antibody	Type	Catalogue no.	Dilution	Vendor
Anti-Pimonidazole	Mouse, mAb	4.3.11.3	1:50	Hypoxyprobe™
CD-31	Rabbit, mAb	77699S	1:100	Cell Signaling

3.7 Western Blot analysis for HIF-1α

Total protein isolation was performed with TRI reagent (Molecular Research Center lnc., Ohio, USA) according to the manufacturer's instructions. 20µg protein was loaded per well and fractionated on 12% SDS-PAGE gel and transferred to PVDF membrane. Membrane was cut to two in order to probe the same membrane for two proteins simultaneously. Membranes were probed with primary antibody specific for HIF-1α and β-actin overnight. Membrane was then incubated with HRP conjugated secondary antibody for an hour. Chemiluminescent signal was detected by SuperSignal™ West Pico PLUS Chemiluminescent Substrate (ThermoFisher Scientific, catalogue # 34578).

Chemiluminescent signal was detected by X-ray film and blot was analysed by ImageJ software.

Table 4. Antibodies used for Western Blot.

Antibody	Type	Catalogue no.	Dilution	Vendor
HIF-1α	Mouse, mAb	sc-13515	1:200	Santa Cruz Inc.
β-actin	Mouse, mAb	ab6276	1:5000	Abcam
Anti-mouse IgG	-	7076	1:3000	Cell signaling

3.8 Statistical analysis

Statistical analysis was done using The GraphPad Prism software (v.6.01; GraphPad Software, Inc., La Jolla, CA, USA). Unpaired Mann-Whitney nonparametric tests were performed in the comparison of sham and mEHT treated groups. Follow-up examinations were statistically evaluated with two-way ANOVA or one-way ANOVA with Tukey correction. Differences were considered statistically significant as *$p < 0.05$, **$p<0.01$, ***$p<0.001$. Data are presented as mean ± SEM.

4. Results

4.1 mEHT induced interstitial blood and capillary damage in TNBC isografts

Untreated tumors had an organized capillary structure, without observable blood in the interstitium. After 5 mEHT treatments a striking observation was large red areas on H&E stained sections. The cause of the red color was the accumulation of red blood cells (RBCs) as identified by high magnification (Fig.5 A). In the same tumors, functional capillaries were characterized as filled with red blood cells in living area of the tumor tissue or surrounded by living cells in comparison to the capillaries in damaged tumor area with no visible red blood cells regarded as dead capillaries (Fig.5 B). The functional capillaries were significantly reduced in mEHT treated tumors as compared to sham tumors (Fig.5 C,D). The reduced number of capillaries was translated to higher RBC covered area. Upon quantification, tumor area covered by RBCs was significantly higher in mEHT treated tumors as compared to sham (Fig.5 E). Similarly, interstitial blood pools were observed 24h after three mEHT treatments in a time-dependent manner. Four-hours post treatment a significant increase in interstitial blood was observed. The interstitial blood covered area peaked at 12h and was significantly reduced at 24h and was further reduced to sham level by 48h-72 after the mEHT treatment (Fig.6 A,B).

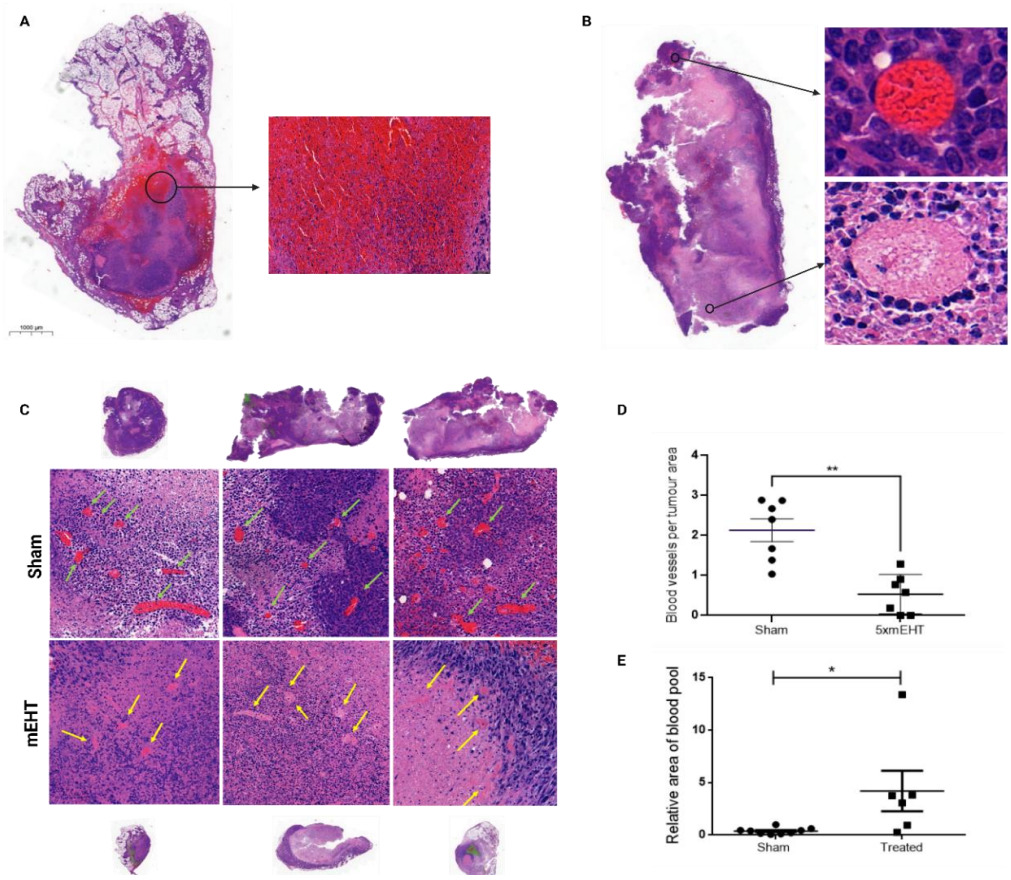

Figure 5: Capillary damage and interstitial blood in TNBC tumors after five mEHT treatments.

(A) A large blood-covered area in 4T07 tumor (Hematoxylin & Eosin staining: 0.9x), erythrocytes between tumor cells in the interstitium (20x). (B) Representative images of red blood cell filled capillary in living area termed functional capillary and dead capillary in the necrotic tumor area (H&E,0.9x,40x). (C) Representative images of tumor samples (H&E, 0.9x,15X), (Pale areas = necrotic, dark areas = composed of living tissue). Green arrows indicate intact capillaries, yellow arrows point at destroyed capillaries. (D) Number of functional capillaries in sham and treated tumors. (E) Relative free blood covered area in sham and treated tumors; unpaired Mann-Whitney test. Mean ± S.E.M, n = 6–12/group,**p=0.0012, *p<0.05.H&E,(0.9X, 20X)

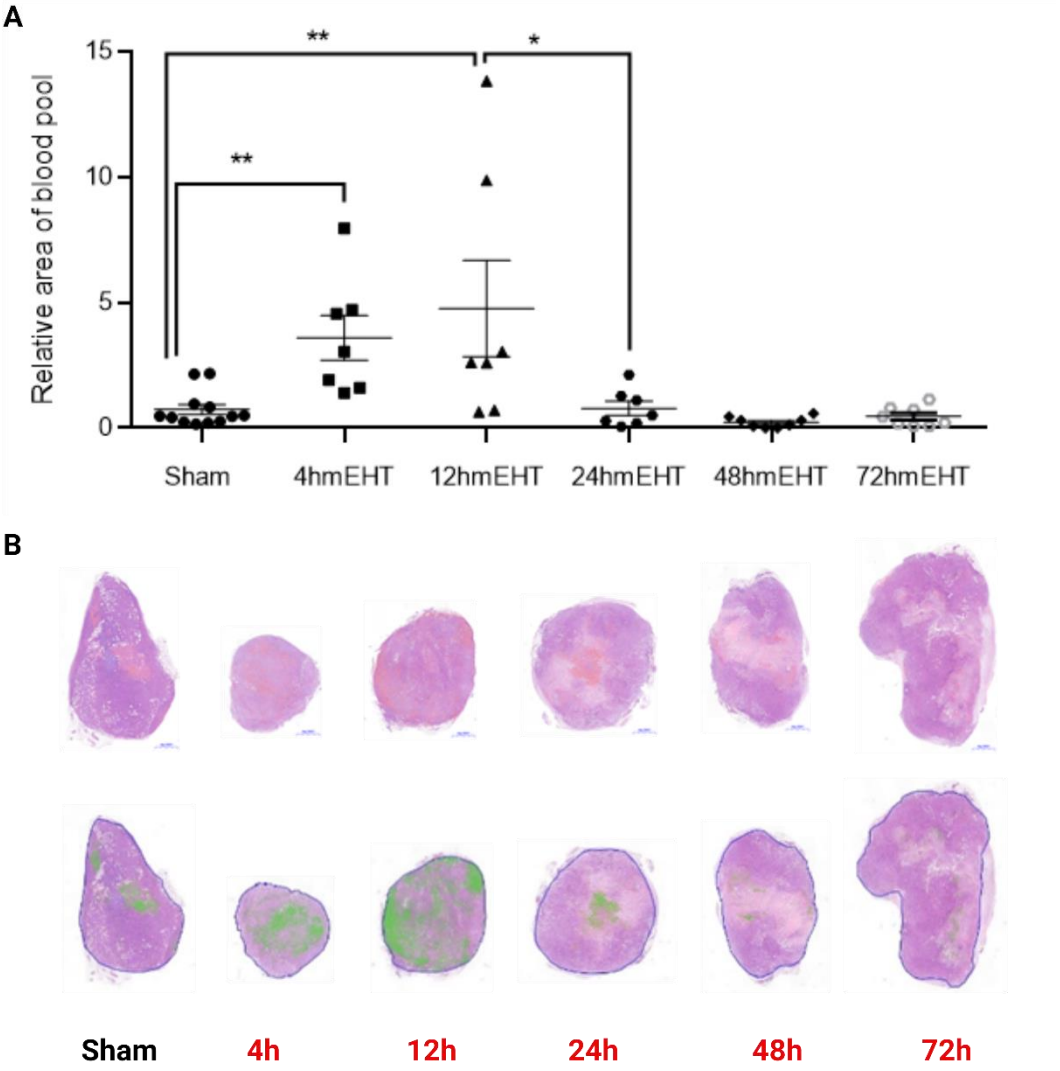

Figure 6: Kinetics of interstitial bleeding after three mEHT treatments. (A) quantification of relative blood covered area on hematoxylin-eosin (H&E) stained 4T1 tumors (1x) (B) Representative images of H&E-stained tumor samples with RBC covered areas masked green; unpaired Mann-Whitney test. Mean ± S.E.M, n = 6–12/group, * p=0.0175, ** p=0.0012, ** p=0.0026.

4.2 mEHT induced capillary damage was accompanied by tumor tissue hypoxia.

Untreated control and sham treated tumors had similar relative mask per tumor area of pimonidazole staining (specific: dark brown/DAB/) in the whole tumor tissue (Fig.7 C). Pimonidazole staining demonstrated significant hypoxia 4 and 12 hours after the last

mEHT treatment. Staining peaked at 24-hours followed by a downward trend reaching sham level by 72 hours (Fig.7 A).

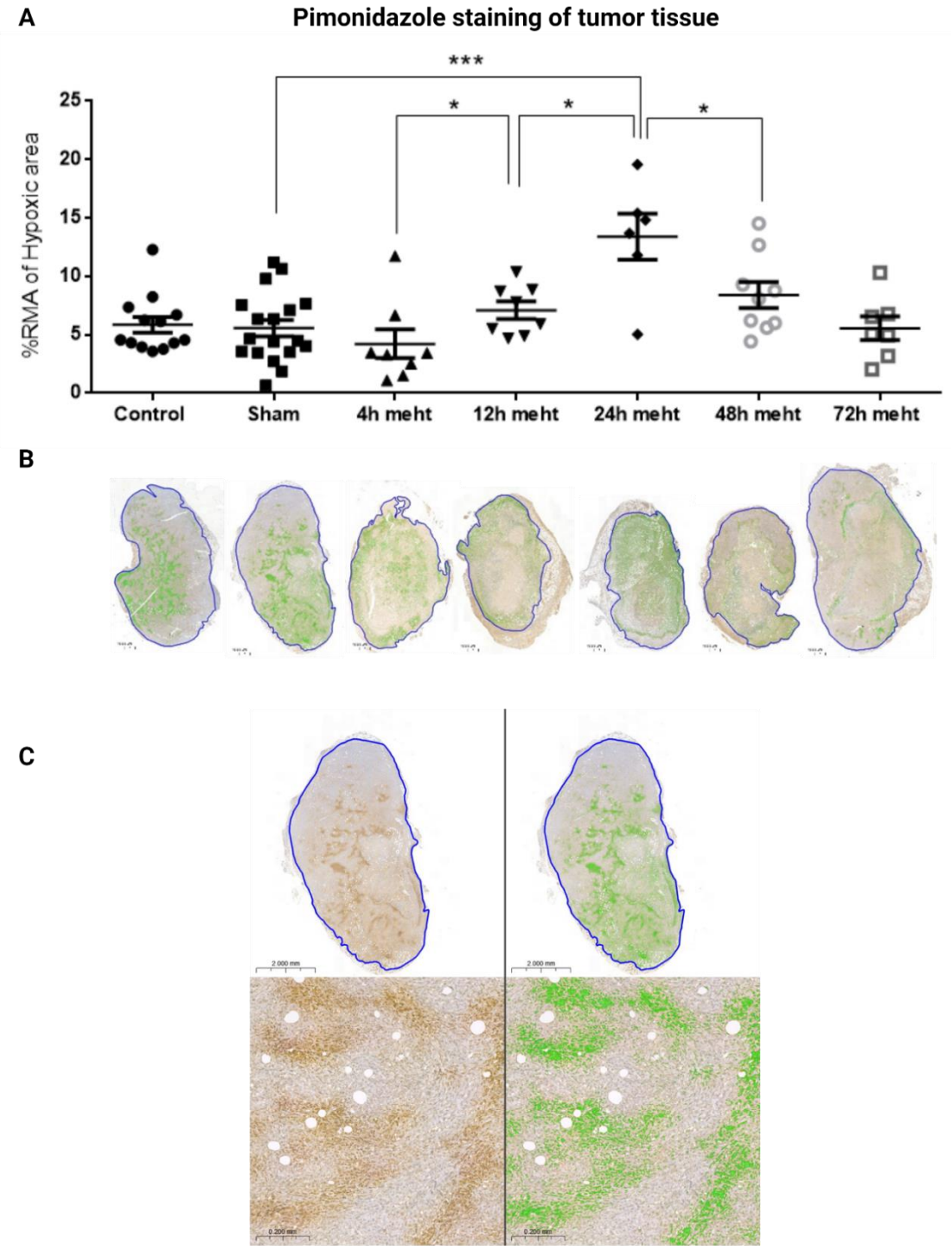

Figure 7: Kinetics of pimonidazole (hypoxia) staining of tumor tissues. (A) Quantification of relative pimonidazole positive area (green masked area within the blue

annotated tumor) in 4T1 tumors. (B) Representative images of stained tumor samples with pimonidazole positive area masked green (0.8x). (C) Representative images for specific staining and masking of pimonidazole stain in histology samples (1x, 10x) RMA: relative mask area. Unpaired Mann-Whitney test. Mean ± S.E.M, n = 6–12/group, * $p<0.05$, *** $p=0.0009$.**2.3**

4.3 Angiogenic repair was initiated in response to mEHT treatment induced hypoxia.

In non-cancerous matrigel implants mEHT treatment resulted in a significant increase of CD45-CD-31+ (endothelial) cells as compared to sham treated matrigel (Fig.8 A). In addition, CD-31 immunohistochemical staining of resected tumor tissues, demonstrated a significant reduction of CD-31 expression at 4 and 12 hours post mEHT, followed by recovery of CD-31 expression at 24-72 hours after the last mEHT treatment (Fig.8 C,D).

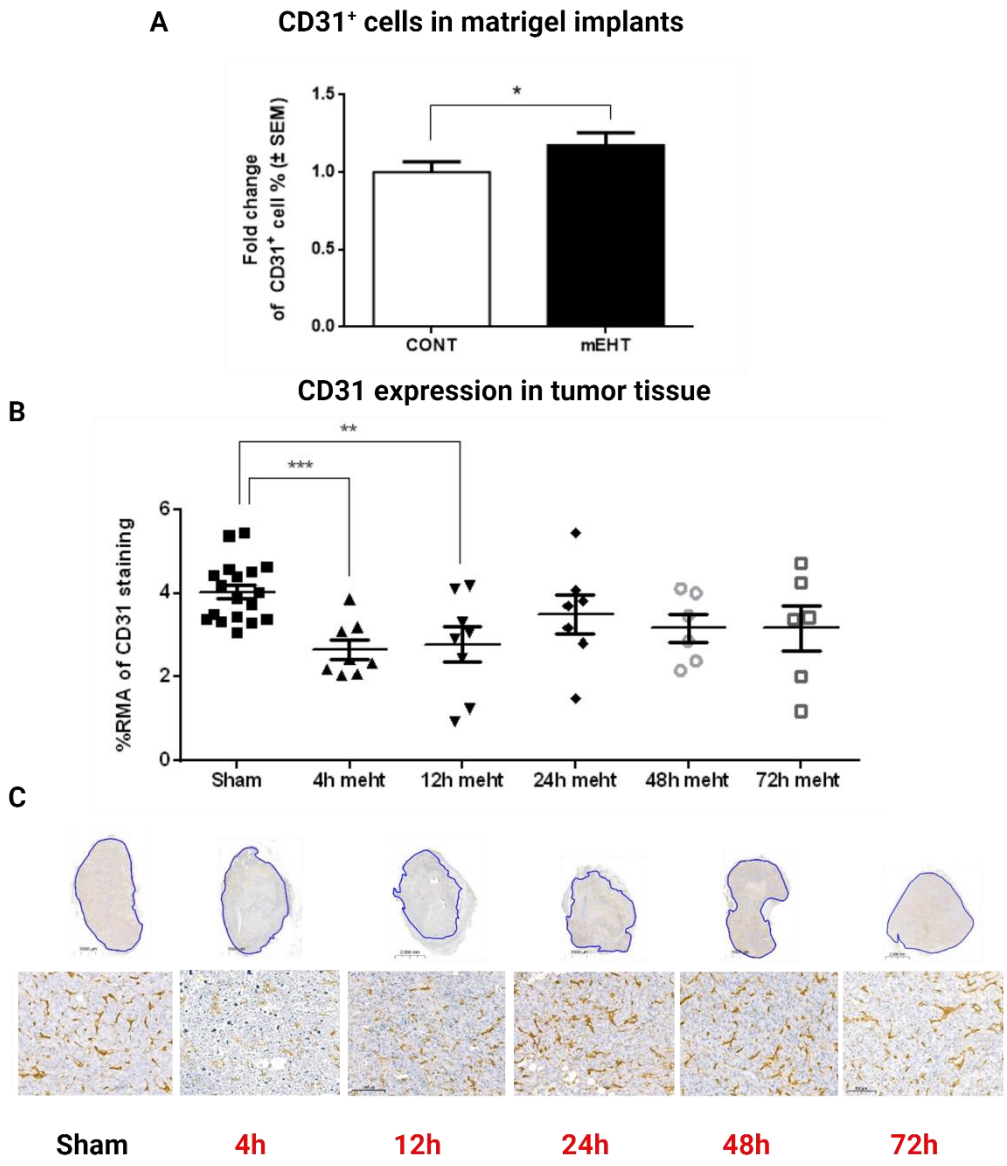

Figure 8: mEHT induced diminution of CD31+ and cells recovered by 24h. (A) Enrichment of CD31+ (blood endothelial cell marker) cells in matrigel in response to mEHT after 24 h. (B) Quantification of relative CD-31 staining in 4T1 tumors. (C) Representative images of stained tumor samples with CD-31-stained area masked green (0.8x), (15x); RMA: relative mask area (green within the blue annotated area on D). (A) Paired t-test *p<0.05. (B) Unpaired Mann-Whitney test. Mean ± S.E.M, n = 6–18/group, ** p=0.004, *** p=0.0002.

4.4 mEHT enhanced anti-tumor potential of drugs

Mice treated with drugs such as digoxin, ASA and SC236 (Fig.9 A,C) did not demonstrate reduction in cancer cell proliferation as the tumor volume remined similar to sham tumors after six and eight days of treatment with respective drugs (Fig 9). mEHT monotherapy however reduced tumor progression after three treatments in one experiment as compared to sham tumors (Fig.9 C). Interestingly, combining digoxin with modulated electrohyperthermia significantly increased the efficacy of the drug in terms of reduced tumor cell proliferation as compared to tumors treated digoxin only after five days of drug administration as compared to sham tumors and mEHT monotherapy (Fig.9 A) and demonstrated a significantly higher tumor volume reduction in combination group as compared to individual mEHT and digoxin monotherapies after eight days of drug administration (Fig.9 B). Similarly, After 6 days of administering ASA and SC236, Combination groups had a significantly lower tumor volume as compared to sham tumors and after eight days of administration mEHT+SC236 group significantly reduced tumor volume as compared to mEHT monotherapy and SC236 monotherapy (Fig.9 C,D).

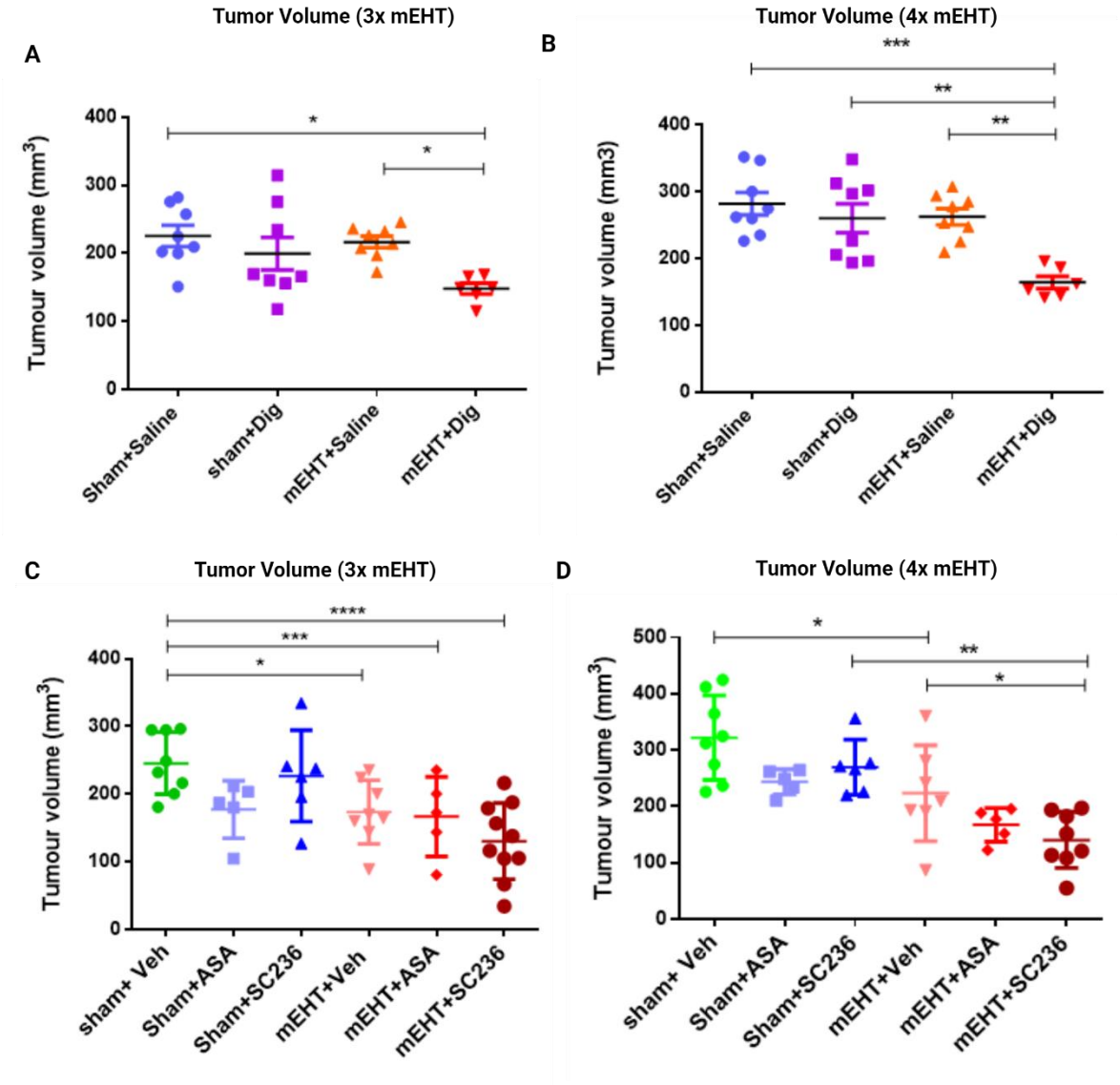

Figure 9: mEHT enhances anti-cancer efficacy of drugs. (A) Tumor volume in mice receiving digoxin after three mEHT treatments. (B) Tumor volume in mice receiving digoxin after four mEHT treatments (C) Tumor volume in mice receiving Aspirin (ASA) and SC236 after three mEHT treatments. (D) Tumor volume in mice receiving Aspirin (ASA) and SC236 after four mEHT treatments. (A) One-way ANOVA, Tukey correction, (A) *p<0.05. (B) One-way ANOVA-Tukey correction, *** p<0.0005, **p<0.005. (C, D) One-way ANOVA-Tukey correction, *p< 0.05; **p< 0.01; ***p< 0.001; ****p< 0.0001.

4.5. Digoxin enhanced the tumor killing effect of mEHT in-vivo

Digoxin did not demonstrate toxicity in mice at 2mg/kg dosage as the body weights of mice in all four groups remained almost same and no mouse lost significant weight during treatment (Fig.10 A) Tumor volume increased constantly in sham+saline treated mice, digoxin monotherapy did not influence tumor volume (Fig.10 B) during the study or tumor weight (Fig.10 C) at the end of the study compared to sham treated tumors. Although, the effects of mEHT monotherapy were not reflected in tumor size (Fig.10 B) mEHT alone did reduce the tumor weight significantly as compared to sham at the end of the study (Fig.10 C). Combined mEHT and digoxin treatment had a significant synergistic effect on tumor weight reduction not only as compared to sham and digoxin monotherapy but also as compared to mEHT monotherapy. (Fig.10 C,D) Correspondingly, digoxin alone could not induce significantly different tumor tissue damage as compared to sham. However, mEHT alone and in combination with digoxin treatment induced a stronger tumor tissue damage compared to sham and digoxin monotherapy. Even though there was a slight difference, combination therapy did not result in significantly different tumor tissue damage as compared to mEHT monotherapy (Fig.10 E).

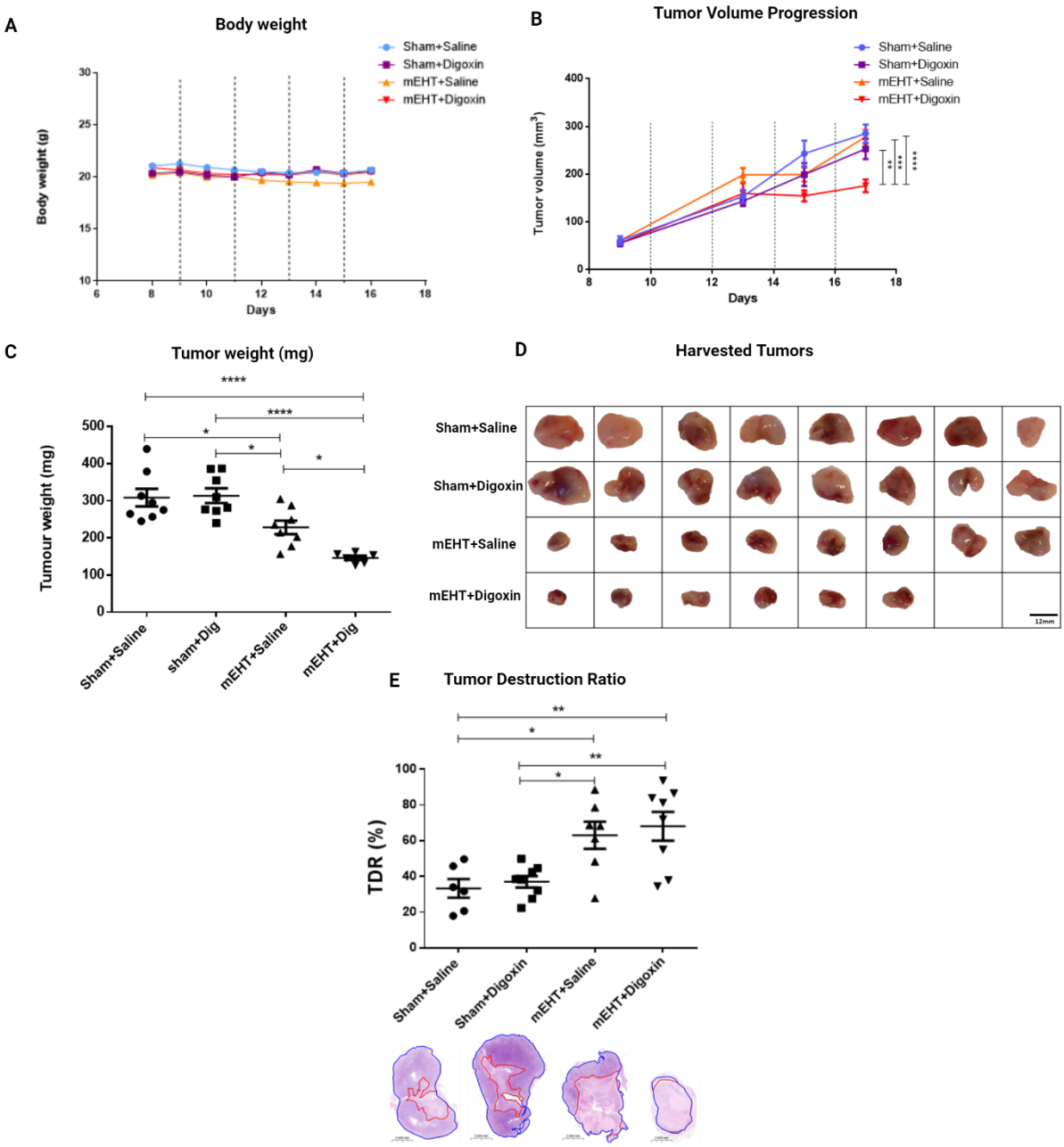

Figure 10: Digoxin provided synergistic tumor growth inhibitory effects when combined with mEHT. (A) Body weights of mice in treatment groups during the course of treatment (dotted lines: mEHT) (B) Tumor volume monitoring by after four treatments (dotted lines) (C) Tumor weight. (D) Representative scale images of the excised 4T1 tumors. (E) TDR: Tumor destruction ratio and representative histology images. (B) Two-way ANOVA, Tukey correction, (A) **p<0.005, ***p=0.001, ****p=<0.0001 (C) One-way ANOVA-Tukey correction, * p<0.05, **** p<0.0001. (E) Scale bar=12mm.(E) One-way Anova-Tukey correction, *p<0.05, **p<0.008.

4.6 Digoxin reduced tissue hypoxia signalling: HIF1-α expression in mEHT treated tumors.

Digoxin alone reduced Hif1-α expression as compared to sham+saline treated tumors. Hif1-α expression increased significantly in mEHT treated tumors as compared to sham+saline and digoxin monotherapy. Combined mEHT+digoxin therapy strongly and significantly reduced HIF1-α expression in contrast to sham, digoxin monotherapy and mEHT monotherapy (Fig.11 A,B).

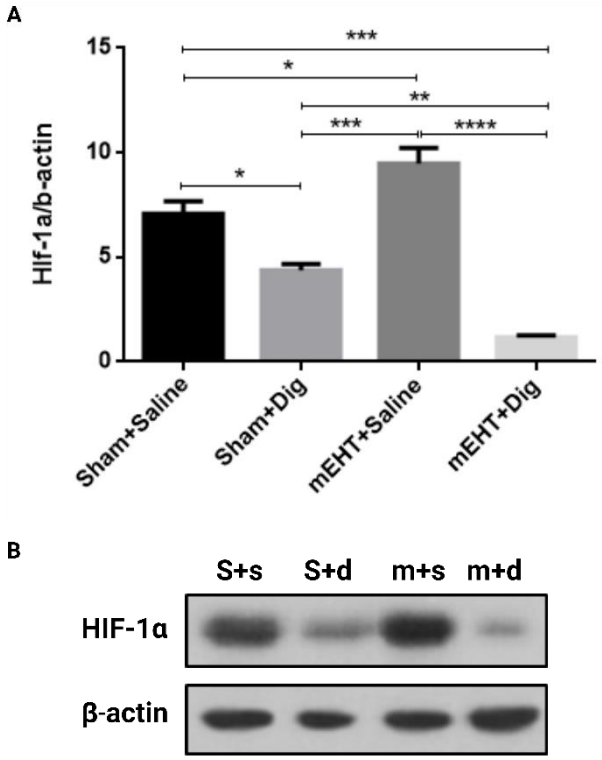

Figure 11: Digoxin reduced tumor hypoxia and angiogenesis when combined with mEHT. (A) Relative fold change of Hif1-α expression as compared to b-actin. (B) Representative images of Western Blot (S+s=Sham+saline, S+d=Sham+digoxin, m+s=mEHT+saline, m+d=mEHT+digoxin) (A) One-way ANOVA, Turkye correction. *p<0.05, **p=0.008, ***p<0.0005, ****p<0.0001.

4.7 Digoxin inhibited blood vessel density in mEHT treated tumors.

Twenty-four hours after last mEHT treatment, CD-31 expression in both sham and mEHT treated tumors were similar as observed before. Similarly, digoxin alone could not significantly inhibit he angiogenic marker expression. However, CD-31 expression was significantly reduced in combined mEHT+digoxin therapy as compared to mEHT monotherapy (Fig.12 A,C).

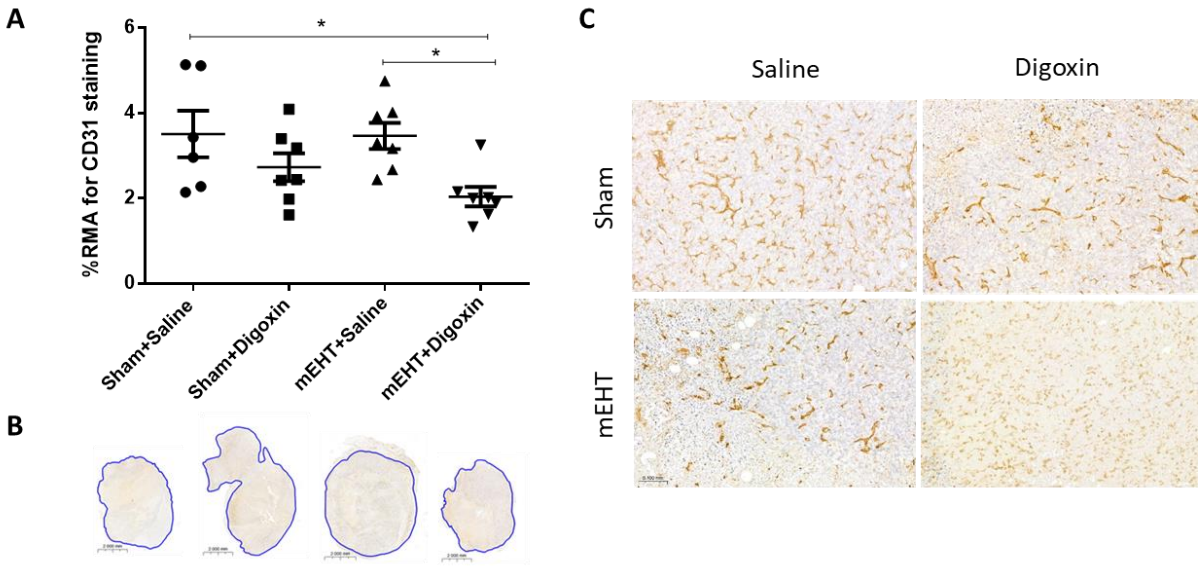

Figure 12: Digoxin reduced vascular density in mEHT treated tumors. (A) Quantification of relative CD-31 staining in tumors. (B,C) Representative images of CD-31 stained tumor samples (B=0.8x, C=15x). (A) One-way ANOVA, Tukey correction, * $p<0.05$.

5. Discussion

We report for the first time our study that investigated tumor hypoxia and related angiogenic repair in cancers subjected to repeated mEHT treatments over a shorter span of time. Owing to the heterogeneous nature of tumor tissue, tumor vasculature is a highly complex mediator of tumor proliferation and dissemination (80, 118). It is also an important determinant to maximize the effects of therapeutic interventions like radiotherapy and chemotherapy (39). Conventional/Whole body hyperthermia (HT) promotes vasodilation and hence increases blood flow to the tumor, which can on one hand facilitates radiation and chemotherapy perfusion while on the other hand promotes tumor growth by providing nutrients and a dissemination route to the tumor cells (50).

Principally, in mEHT, the local heating of the tumor tissue is achieved by energy absorption while the blood flowing through the tumor at physiological temperature acts as a cooling agent. Interestingly in case of loco-regional hyperthermia such as mEHT, the energy absorption i.e. heating and the dissipation by flowing blood is independent. Therefore, a dynamic balance yet a constant small temperature gradient result in heterogenic heating that represents the heterogeneous tumor vasculature (84). This heterogeneous heating therefore provides better cytotoxic effects.

In clinical settings, patients receive multiple mEHT treatments. i.e. an average of 28-30 sessions during treatment (67, 68). In a clinical study, mEHT treatment 3 times a week in combination with concurrent chemotherapy provided a better therapy response and increased disease-free survival in patients with lymph-node metastasis in locally advanced cervical cancer patients (67). Similarly, mEHT in combination with chemotherapy provided better overall survival in cervical cancer patients (68). Since mEHT dosage depends on the specific energy absorbed over the course of treatment (84) the minor temperature difference between the tumor tissue and its vasculature can accumulatively be of significant clinical value. It was therefore clinically relevant to investigate how tumor vasculature responds to repeated mEHT treatments.

Tumor vascularization and oxygenation response to hyperthermia are variable and complex. Effects of HT on blood flow and vascular damage have been extensively researched (145). However, the effect of mEHT on blood flow and vascular damage still

needs investigation. Although mild HT has been reported to promote tumor re-oxygenation (25, 63, 134, 149). Other studies report a reduction in tumor oxygenation due to vascular damage 45 or transient re-oxygenation (49). Furthermore, the relationship between blood perfusion and oxygenation of the tumor tissue is not linear 24 hours after HT (150). Interestingly, tumors subjected to HT for a cumulatively higher time/dosage experience hypoxia and vascular damage which is in line with our findings (Fig. 3,4) (134, 135). Furthermore, we also observed vascular recovery in our cancer model after 24 hours (Fig. 1,4). Our results demonstrate that hypoxia peaked at 24h after mEHT (Fig. 4) as compared to sham tumors which is in line with previous studies (90). However, these findings are different from Kim et al., who compared the effects of mEHT and conventional HT. They observed a small reduction in hypoxia after mEHT (60) which could be due to two reasons. Firstly, Kim et al., treated tumors with mEHT only once while we did multiple mEHT treatments. Secondly, the tumors were harvested 72 hours not 24 hours after mEHT by the former group. In line with Kim et al., findings we also observed reduction in hypoxia at 72h time point as well.

As it is already reported that mEHT elicits stress responses in cancer (16, 24, 28, 61, 114, 143, 158) we hypothesized that tissue hypoxia is triggering another stress response which is translated to angiogenic repair. A significant upregulation in CD-31+ & CD-45- endothelial cells 24 hours after last mEHT treatment in matrigel implants strengthened our hypothesis. Furthermore, our time kinetics study demonstrated a reduction in expression of vascular endothelial markers, CD105 and CD-31 after 12 hours followed by recovery in expression after 24 hours of mEHT treatment which endorses our hypothesis. Additionally, in a multiplex analysis of mEHT-treated tumors (114), we found previously a number of genes including *Hap*toglobin *(Hp)*, *V*ascular *E*ndothelial *G*rowth *F*actor- *D (VEGF-D)*, *Pleiotropin (Ptn)*, *BMP*-binding *E*ndothelial *R*egulator *(BMPER)*, and chemokine (*C-X-C* motif) *l*igand-12 (*CXCL-12*) with significantly high overexpression. Furthermore, based on Gene Ontology analysis on our aforementioned multiplex analysis (114), fourteen genes involved in vascular development (Fig.13 A) were modulated in response to mEHT treatment. Roles of these genes as angiogenic activators in response to hypoxic stress have already been established in brain, cardiac, kidney, and cancer cells (22, 30, 43, 59, 74, 112, 137, 140, 146, 164). We therefore believe that these genes facilitate angiogenesis by modulating one or more steps of it (Fig.13 C).

A

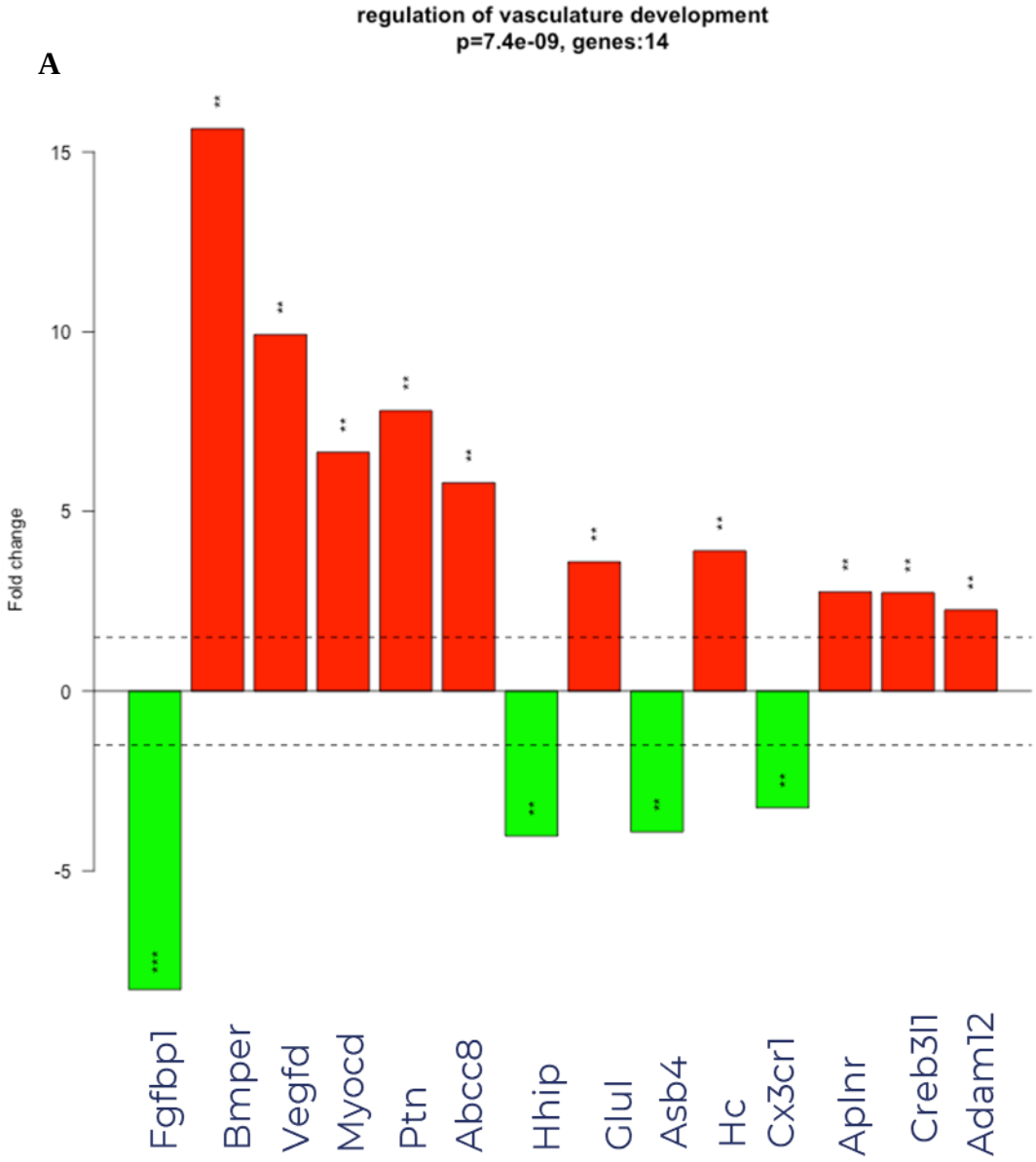
regulation of vasculature development
p=7.4e-09, genes:14
Fold change
15
10
5
0
-5
Fgfbp1
Bmper
Vegfd
Myocd
Ptn
Abcc8
Hhip
Glul
Asb4
Hc
Cx3cr1
Aplnr
Creb3l1
Adam12

B

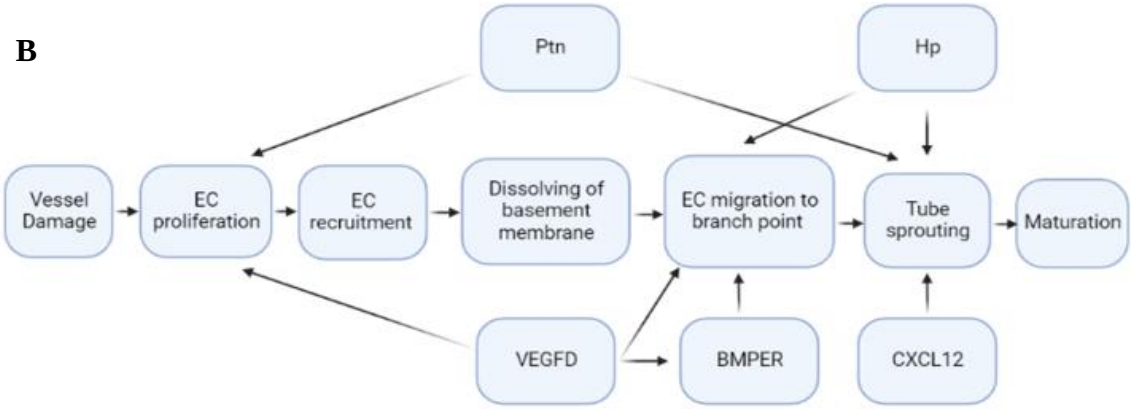
Ptn
Hp
Vessel Damage
EC proliferation
EC recruitment
Dissolving of basement membrane
EC migration to branch point
Tube sprouting
Maturation
VEGFD
BMPER
CXCL12

Figure 13: Vascular genes upregulated in response to mEHT in 4T1 model of TNBC. **(**A) Gene ontology of multiplex analysis of 4T1 tumors highlighted fourteen genes modulated in response to mEHT involved in the regulation of vascular development (114). (B) A theoretical network of genes upregulated in 4T1 model in stress responsive vascular development (22, 30, 43, 59, 74, 112, 114, 137, 140, 146, 164).

Table 5: Cellular stress response related genes, upregulated by mEHT treatment as detected by different multiplex assays (next generation sequencing (NGS), Nanostring.

Nr.	Gene name	Description	NGS		Nanostring	
statistics			FC	p	FC	p
1	Bmper	BMP-binding endothelial regulator	15.65	0.00042	No DE	
2	Hp	haptoglobin	9.7	0.0002	7.5	2.5E-04
3	VEGFD	vascular endothelial growth factor D	9.9	0.0030	15.7	2.59E-05
4	Ptn	Pleiotropin	7.8	0.0099	7.6	8.2E-04
5	CXCL12	chemokine (C-X-C motif) ligand 12	6.80	0.0016	No DE	

We aimed to inhibit hypoxia signalling with the cardiac glycoside digoxin. It is noteworthy that in the literature, digoxin had been administered for 14-40 days at a concentration of 2mg/kg daily and needed an average of 21 days of treatment alone or in

combination with other chemotherapeutics to observe significant tumor volume reduction. Gayed et al, however administered digoxin only for 7 days and could observe significant reduction of HIF1-α and CD-31 expression but they could not describe any significant reduction in tumor growth over this short treatment period (38). We, for the first time, observed significant tumor weight reduction by day 8 of digoxin administration when combined with mEHT treatment, hence mEHT accelerated the anticancer effects of digoxin. Furthermore, we observed a reduction in Hif1-α expression hence hypoxia signalling and inhibition of angiogenesis in tumors subjected to combination therapy.

The data is of valuable importance as the results have dual interpretations. Our data explicate a collaborative relationship between mEHT and digoxin. The combination can provide better outcomes by mEHT enhancing digoxin functionality; reducing tumor weight over a shorter span of time, and digoxin reducing the hypoxic and angiogenic response initiated by repeated mEHT. Similarly, mEHT significantly increased the efficacy of SC-236 as compared to SC-236 alone. Further research on downstream targets of Hif1-α modulated in response to combined digoxin and mEHT would be of valuable importance. In conclusion, our findings corroborate the efficiency of mEHT both as a complementary treatment and monotherapy in our TNBC model. We for the first time reported an elaborate time-related vascular and hypoxic response to repeated mEHT treatments. Furthermore, our findings substantiate the role of digoxin as an anti-cancer therapy that could reduce hypoxia, angiogenesis and tumor growth over a shorter treatment regimen when combined with mEHT. We believe combining mEHT with digoxin can provide better results over a shorter span of time in clinical settings.

6. Conclusions

The studies mentioned in this dissertation investigated the molecular basis of stress responses initiated in response to modulated electrohyperthermia in triple negative breast cancer. The main findings demonstrated that:

1. Repeated modulated electrohyperthermia (mEHT) induced vascular damage in triple negative breast cancer models.
2. mEHT mediated vascular damage triggers hypoxia in a time dependant manner.
3. mEHT promotes proliferation of $CD31^{+}$ endothelial cells in non-cancerous matrigel implants.
4. An angiogenic repair is initiated in response to mEHT in a time related manner.
5. Digoxin can be repurposed as an anticancer drug as it reduces tumor proliferation and HIF1-α expression.
6. Combining mEHT with anti-cancer drugs (digoxin, SC-236) slows tumor proliferation in a short period of time as compared to monotherapy at the same dosage.
7. Combination therapy (mEHT+digoxin) has synergistic anti-tumor effects.

7. Summary

We observed severe vascular damage in mEHT-treated tumors and investigated the potential synergism between mEHT and inhibition of tumor vasculature recovery in our TNBC mouse model. We further investigated the efficacy of mEHT in enhancing the effectiveness of drugs with anti-cancer ability such as HIF1-α inhibiting digoxin and/or COX-2 inhibitors; SC-236. mEHT induced vascular damage four to twelve hours after treatment leading to tissue hypoxia detected at twenty-four hours. Hypoxia in treated tumors induced an angiogenic recovery twenty-four hours after the last treatment. Administration of the cardiac glycoside digoxin could synergistically augment mEHT-mediated tumor damage and could reduce tissue hypoxia (HIF1-α) and consequent vascular recovery in mEHT-treated TNBC tumors. Similarly, mEHT enhanced efficacy of digoxin and SC-236 as anti-cancer agents, demonstrating an early response in combination with mEHT as compared to drug monotherapy.

8. **References**

1. Potentiation of Cisplatin-based Chemotherapy by Digoxin in Advanced Unresectable Head and Neck Cancer Patients. https://ClinicalTrials.gov/show/NCT02906800.

2. Neoadjuvant Concomitant Modulated Electro-hyperthermia in HER2-negative Breast Cancer. https://classic.clinicaltrials.gov/show/NCT05889390.

3. DIG-HIF-1 Pharmacodynamic Trial in Newly Diagnosed Operable Breast Cancer. https://ClinicalTrials.gov/show/NCT01763931.

4. A Study to Evaluate the Effect of Multiple Doses of Enzalutamide on the Pharmacokinetics of Substrates of P-glycoprotein (Digoxin) and Breast Cancer Resistant Protein (Rosuvastatin) in Male Subjects With Prostate Cancer. https://ClinicalTrials.gov/show/NCT04094519.

5. Digoxin for Recurrent Prostate Cancer. https://ClinicalTrials.gov/show/NCT01162135.

6. Phase IB Metformin, Digoxin, Simvastatin in Solid Tumors. https://ClinicalTrials.gov/show/NCT03889795.

7. FOLFIRINOX With Digoxin in Patients With Resectable Pancreatic Cancer. https://ClinicalTrials.gov/show/NCT04141995.

8. Digoxin for the Reinduction of Radioiodine Uptake in Metastatic or Locally Advanced Non-medullary Thyroid Carcinoma. https://ClinicalTrials.gov/show/NCT05507775.

9. Phase II Multicentric Study of Digoxin Per os in Classic or Endemic Kaposi' s Sarcoma. https://ClinicalTrials.gov/show/NCT02212639.

10. Digoxin Induced Dissolution of CTC Clusters. https://ClinicalTrials.gov/show/NCT03928210.

11. A Phase 1B Clinical Trial of Trametinib Plus Digoxin in Patients With Unresectable or Metastatic BRAF Wild-type Melanoma. https://ClinicalTrials.gov/show/NCT02138292.

12. Abud EM, Maylor J, Undem C, Punjabi AN, Zaiman A, Myers AC, Sylvester JJ, Semenza GL, Shimoda LA. Digoxin Inhibits Development of Hypoxic Pulmonary Hypertension in Mice. Proceedings of the National Academy of Sciences. 2012.

13. Ademaj A, Veltsista DP, Ghadjar P, Marder D, Oberacker E, Ott OJ, Wust P, Puric E, Hälg RA, Rogers S, Bodis S, Fietkau R, Crezee H, Riesterer O. Clinical Evidence for Thermometric Parameters to Guide Hyperthermia Treatment. Cancers. 2022;14(3):625.

14. Al-Ostoot FH, Salah S, Khamees HA, Khanum SA. Tumor angiogenesis: Current challenges and therapeutic opportunities. Cancer Treatment and Research Communications. 2021;28:100422.

15. Alshaibi HF, Al-Shehri B, Hassan B, Al-Zahrani R, Assiss T. Modulated Electrohyperthermia: A New Hope for Cancer Patients. BioMed Research International. 2020;2020.

16. Andocs G, Meggyeshazi N, Balogh L, Spisak S, Maros ME, Balla P, Kiszner G, Teleki I, Kovago C, Krenacs T. Upregulation of heat shock proteins and the promotion of damage-associated molecular pattern signals in a colorectal cancer model by modulated electrohyperthermia. Cell Stress and Chaperones. 2015;20:37-46.

17. Andocs G, Rehman M, Zhao Q, Tabuchi Y, Kanamori M, Kondo T. Comparison of biological effects of modulated electro-hyperthermia and conventional heat treatment in human lymphoma U937 cells. Cell death discovery. 2016;2(1):1-10.

18. Arnold M, Morgan E, Rumgay H, Mafra A, Singh D, Laversanne M, Vignat J, Gralow JR, Cardoso F, Siesling S, Soerjomataram I. Current and future burden of breast cancer: Global statistics for 2020 and 2040. The Breast. 2022;66:15-23.

19. Aslakson CJ, Miller FR. Selective events in the metastatic process defined by analysis of the sequential dissemination of subpopulations of a mouse mammary tumor. Cancer research. 1992;52(6):1399-405.

20. Attalla S, Taifour T, Muller W. Tailoring therapies to counter the divergent immune landscapes of breast cancer. Frontiers in Cell and Developmental Biology. 2023;11:1111796.

21. Baritaud M, Boujrad H, Lorenzo HK, Krantic S, Susin SA. Histone H2AX: The missing link in AIF-mediated caspase-independent programmed necrosis. Cell cycle. 2010;9(16):3186-93.

22. Başyiğit F, Karayiğit O, Nurkoç SG, Duyuler S, Duyuler PT. Association of Serum Pleiotrophin Levels with Acute Coronary Syndrome. 2022.

23. Bertagnolli MM, Eagle CJ, Zauber AG, Redston M, Solomon SD, Kim K, Tang J, Rosenstein RB, Wittes J, Corle D. Celecoxib for the prevention of sporadic colorectal adenomas. New England Journal of Medicine. 2006;355(9):873-84.

24. Besztercei B, Vancsik T, Benedek A, Major E, Thomas MJ, Schvarcz CA, Krenács T, Benyó Z, Balogh A. Stress-induced, p53-mediated tumor growth inhibition of melanoma by modulated electrohyperthermia in mouse models without major immunogenic effects. International Journal of Molecular Sciences. 2019;20(16):4019.

25. Brizel DM, Scully SP, Harrelson JM, Layfield LJ, Dodge RK, Charles HC, Samulski TV, Prosnitz LR, Dewhirst MW. Radiation therapy and hyperthermia improve the oxygenation of human soft tissue sarcomas. Cancer Res. 1996;56(23):5347-50.

26. Burd R, Dziedzic TS, Xu Y, Caligiuri MA, Subjeck JR, Repasky EA. Tumor cell apoptosis, lymphocyte recruitment and tumor vascular changes are induced by low temperature, long duration (fever-like) whole body hyperthermia. Journal of cellular physiology. 1998;177(1):137-47.

27. Choi E, Jung B, Lee S, Yoo H, Shin E, Ko H, Chang S, Kim S, Jeon S. A clinical drug library screen identifies clobetasol propionate as an NRF2 inhibitor with potential therapeutic efficacy in KEAP1 mutant lung cancer. Oncogene. 2017;36(37):5285-95.

28. Danics L, Schvarcz CA, Viana P, Vancsik T, Krenács T, Benyó Z, Kaucsár T, Hamar P. Exhaustion of Protective Heat Shock Response Induces Significant Tumor Damage by Apoptosis after Modulated Electro-Hyperthermia Treatment of Triple Negative Breast Cancer Isografts in Mice. Cancers (Basel). 2020;12(9).

29. Derakhshan F, Reis-Filho JS. Pathogenesis of triple-negative breast cancer. Annual Review of Pathology: Mechanisms of Disease. 2022;17:181-204.

30. Ding P, Chen W, Yan X, Zhang J, Li C, Zhang G, Wang Y, Li Y. BMPER alleviates ischemic brain injury by protecting neurons and inhibiting neuroinflammation via Smad3-Akt-Nrf2 pathway. CNS Neuroscience & Therapeutics. 2022;28(4):593-607.

31. do Nascimento RG, Otoni KM. Histological and molecular classification of breast cancer: what do we know? Mastology. 2020;30:1-8.

32. Dong W, Peng J, Gao H, Li H, Liu D, Tan Y, Zhang T. Digoxin Downregulates NDRG1 and VEGF Through the Inhibition of HIF-1α Under Hypoxic Conditions in Human Lung Adenocarcinoma A549 Cells. International Journal of Molecular Sciences. 2013.

33. Fiorentini G, Sarti D, Casadei V, Milandri C, Dentico P, Mambrini A, Nani R, Fiorentini C, Guadagni S. Modulated electro-hyperthermia as palliative treatment for pancreatic cancer: a retrospective observational study on 106 patients. Integrative Cancer Therapies. 2019;18:1534735419878505.

34. Fiorentini G, Sarti D, Ranieri G, Gadaleta CD, Fiorentini C, Milandri C, Mambrini A, Guadagni S. Modulated electro-hyperthermia in stage III and IV pancreatic cancer: Results of an observational study on 158 patients. World Journal of Clinical Oncology. 2021;12(11):1064.

35. Firatligil-Yildirir B, Yalcin-Ozuysal O, Nonappa N. Recent advances in lab-on-a-chip systems for breast cancer metastasis research. Nanoscale Advances. 2023.

36. Forika G, Balogh A, Vancsik T, Zalatnai A, Petovari G, Benyo Z, Krenacs T. Modulated electro-hyperthermia resolves radioresistance of Panc1 pancreas adenocarcinoma and promotes DNA damage and apoptosis in vitro. International journal of molecular sciences. 2020;21(14):5100.

37. Fragkos M, Jurvansuu J, Beard P. H2AX is required for cell cycle arrest via the p53/p21 pathway. Molecular and cellular biology. 2009;29(10):2828-40.

38. Gayed BA, O'Malley KJ, Pilch J, Wang Z. Digoxin inhibits blood vessel density and HIF-1a expression in castration-resistant C4-2 xenograft prostate tumors. Clin Transl Sci. 2012;5(1):39-42.

39. Graham K, Unger E. Overcoming tumor hypoxia as a barrier to radiotherapy, chemotherapy and immunotherapy in cancer treatment. Int J Nanomedicine. 2018;13:6049-58.

40. Gray R, Bradley R, Braybrooke J, Davies C, Pan H, editors. Increasing the dose intensity of adjuvant chemotherapy: an EBCTCG meta-analysis. San Antonio Breast Cancer Symposium; 2017.

41. Guy A. Physical aspects of localized heating by radio-waves and microwaves. Hyperthermia in cancer therapy. 1983:279-304.

42. Gy V, Szigeti GP, Andocs G, Szasz A. Nanoheating without artificial nanoparticles. 2015.

43. Hamar P. A New Role of Acute Phase Proteins: Local Production Is an Ancient, General Stress-Response System of Mammalian Cells. International Journal of Molecular Sciences. 2022;23(6):2972.

44. Harbeck N, Penault-Llorca F, Cortes J, Gnant M, Houssami N, Poortmans P, Ruddy K, Tsang J, Cardoso F. Breast cancer. Nature Reviews Disease Primers. 2019;5(1):66.

45. Hashemi Goradel N, Najafi M, Salehi E, Farhood B, Mortezaee K. Cyclooxygenase-2 in cancer: A review. J Cell Physiol. 2019;234(5):5683-99.

46. He L, Lv Y, Song Y, Zhang B. The prognosis comparison of different molecular subtypes of breast tumors after radiotherapy and the intrinsic reasons for their distinct radiosensitivity. Cancer management and research. 2019:5765-75.

47. Hildebrandt B, Wust P, Ahlers O, Dieing A, Sreenivasa G, Kerner T, Felix R, Riess H. The cellular and molecular basis of hyperthermia. Critical Reviews in Oncology/Hematology. 2002;43(1):33-56.

48. Hong R, Xu B. Breast cancer: an up-to-date review and future perspectives. Cancer Communications. 2022;42(10):913-36.

49. Horsman M, Overgaard J. Hot topic: Can mild hyperthermia improve tumour oxygenation? International journal of hyperthermia. 1997;13(2):141-7.

50. Horsman MR, Overgaard J. Hyperthermia: a Potent Enhancer of Radiotherapy. Clinical Oncology. 2007;19(6):418-26.

51. Hou Y-Q, Wang Y-Y, Wang X-C, Liu Y, Zhang C-Z, Chen Z-S, Zhang Z, Wang W, Kong D-X. Multifaceted anti-colorectal tumor effect of digoxin on HCT8 and SW620 cells in vitro. Gastroenterology Report. 2020;8(6):465-75.

52. Hua H, Zhang H, Kong Q, Wang J, Jiang Y. Complex roles of the old drug aspirin in cancer chemoprevention and therapy. Medicinal research reviews. 2019;39(1):114-45.

53. Huber SM. Oncochannels. Cell calcium. 2013;53(4):241-55.

54. Jeon T-W, Yang H, Lee CG, Oh ST, Seo D, Baik IH, Lee EH, Yun I, Park KR, Lee Y-H. Electro-hyperthermia up-regulates tumour suppressor Septin 4 to induce apoptotic cell death in hepatocellular carcinoma. International Journal of Hyperthermia. 2016;32(6):648-56.

55. Joseph JV, Conroy S, Pavlov KV, Sontakke P, Tomar T, Eggens-Meijer E, Balasubramaniyan V, Wagemakers M, Dunnen WFAd, Kruyt FAE. Hypoxia Enhances Migration and Invasion in Glioblastoma by Promoting a Mesenchymal Shift Mediated by the HIF1α–ZEB1 Axis. Cancer Letters. 2015.

56. Kao PH-J, Chen C-H, Tsang Y-W, Lin C-S, Chiang H-C, Huang C-C, Chi M-S, Yang K-L, Li W-T, Kao S-J. Relationship between energy dosage and apoptotic cell death by modulated electro-hyperthermia. Scientific reports. 2020;10(1):8936.

57. Kerr AJ, Dodwell D, McGale P, Holt F, Duane F, Mannu G, Darby SC, Taylor CW. Adjuvant and neoadjuvant breast cancer treatments: A systematic review of their effects on mortality. Cancer treatment reviews. 2022;105:102375.

58. Kim S, Lee JH, Cha J, You SH. Beneficial effects of modulated electro-hyperthermia during neoadjuvant treatment for locally advanced rectal cancer. International Journal of Hyperthermia. 2021;38(1):144-51.

59. Kim S, Yeo MK, Kim JS, Kim JY, Kim KH. Elevated CXCL12 in the plasma membrane of locally advanced rectal cancer after neoadjuvant chemoradiotherapy: a potential prognostic marker. J Cancer. 2022;13(1):162-73.

60. Kim W, Kim M-S, Kim H-j, Lee E, Jeong J-h, Park I, Jeong YK, Jang WI. Role of HIF-1α in response of tumors to a combination of hyperthermia and radiation in vivo. International Journal of Hyperthermia. 2018;34(3):276-83.

61. Krenacs T, Meggyeshazi N, Forika G, Kiss E, Hamar P, Szekely T, Vancsik T. Modulated Electro-Hyperthermia-Induced Tumor Damage Mechanisms Revealed in Cancer Models. International Journal of Molecular Sciences. 2020;21(17):6270.

62. Lasso P, Llano Murcia M, Sandoval TA, Urueña C, Barreto A, Fiorentino S. Breast Tumor Cells Highly Resistant to Drugs Are Controlled Only by the Immune Response Induced in an Immunocompetent Mouse Model. Integr Cancer Ther. 2019;18:1534735419848047.

63. Lee S-Y, Kim J-H, Han Y-H, Cho D-H. The effect of modulated electro-hyperthermia on temperature and blood flow in human cervical carcinoma. International Journal of Hyperthermia. 2018;34(7):953-60.

64. Lee S-Y, Lorant G, Grand L, Szasz AM. The Clinical Validation of Modulated Electro-Hyperthermia (mEHT). Cancers. 2023;15(18):4569.

65. Lee S-Y, Szigeti GP, Szasz AM. Oncological hyperthermia: The correct dosing in clinical applications. International Journal of Oncology. 2019;54(2):627-43.

66. Lee SY, Kim M-G. The effect of modulated electro-hyperthermia on the pharmacokinetic properties of nefopam in healthy volunteers: A randomised, single-dose, crossover open-label study. International Journal of Hyperthermia. 2015;31(8):869-74.

67. Lee SY, Lee DH, Cho DH. Modulated electrohyperthermia in locally advanced cervical cancer: Results of an observational study of 95 patients. Medicine (Baltimore). 2023;102(3):e32727.

68. Lee SY, Lee NR, Cho DH, Kim JS. Treatment outcome analysis of chemotherapy combined with modulated electro-hyperthermia compared with chemotherapy alone for recurrent cervical cancer, following irradiation. Oncology letters. 2017;14(1):73-8.

69. Lehmann BD, Bauer JA, Chen X, Sanders ME, Chakravarthy AB, Shyr Y, Pietenpol JA. Identification of human triple-negative breast cancer subtypes and preclinical models for selection of targeted therapies. The Journal of clinical investigation. 2011;121(7):2750-67.

70. Lehmann BD, Jovanović B, Chen X, Estrada MV, Johnson KN, Shyr Y, Moses HL, Sanders ME, Pietenpol JA. Refinement of triple-negative breast cancer molecular subtypes: implications for neoadjuvant chemotherapy selection. PloS one. 2016;11(6):e0157368.

71. Lichtenberger LM. Using aspirin to prevent and treat cancer. Inflammopharmacology. 2024;32(1):903-8.

72. Liu B, Qu L, Yan S. Cyclooxygenase-2 promotes tumor growth and suppresses tumor immunity. Cancer Cell International. 2015;15(1):106.

73. Liu C, Wu P, Zhang A, Mao X. Advances in rodent models for breast cancer formation, progression, and therapeutic testing. Frontiers in Oncology. 2021;11:593337.

74. Liu SQ, Tefft BJ, Roberts DT, Zhang LQ, Ren Y, Li YC, Huang Y, Zhang D, Phillips HR, Wu YH. Cardioprotective proteins upregulated in the liver in response to experimental myocardial ischemia. Am J Physiol Heart Circ Physiol. 2012;303(12):H1446-58.

75. Loi S, Sirtaine N, Piette F, Salgado R, Viale G, Van Eenoo F, Rouas G, Francis P, Crown J, Hitre E. Prognostic and predictive value of tumor-infiltrating lymphocytes in a phase III randomized adjuvant breast cancer trial in node-positive breast cancer comparing the addition of docetaxel to doxorubicin with doxorubicin-based chemotherapy: BIG 02-98. J Clin Oncol. 2013;31(7):860-7.

76. Lu H, Samanta D, Xiang L, Zhang H, Hu H, Chen I, Bullen JW, Semenza GL. Chemotherapy Triggers HIF-1–dependent Glutathione Synthesis and Copper Chelation That Induces the Breast Cancer Stem Cell Phenotype. Proceedings of the National Academy of Sciences. 2015.

77. Lu H, Tran TTV, Park Y, Chen I, Lan J, Xie Y, Semenza GL. Reciprocal Regulation of DUSP9 and DUSP16 Expression by HIF1 Controls ERK and P38 MAP Kinase Activity and Mediates Chemotherapy-Induced Breast Cancer Stem Cell Enrichment. Cancer Research. 2018.

78. Lugano R, Ramachandran M, Dimberg A. Tumor angiogenesis: causes, consequences, challenges and opportunities. Cellular and Molecular Life Sciences. 2020;77(9):1745-70.

79. Maishi N, Annan DA, Kikuchi H, Hida Y, Hida K. Tumor endothelial heterogeneity in cancer progression. Cancers. 2019;11(10):1511.

80. Majidpoor J, Mortezaee K. Angiogenesis as a hallmark of solid tumors-clinical perspectives. Cellular Oncology. 2021;44(4):715-37.

81. Masuda N, Lee S-J, Ohtani S, Im Y-H, Lee E-S, Yokota I, Kuroi K, Im S-A, Park B-W, Kim S-B. Adjuvant capecitabine for breast cancer after preoperative chemotherapy. New England Journal of Medicine. 2017;376(22):2147-59.

82. McDonald M, Corde S, Lerch M, Rosenfeld A, Jackson M, Tehei M. First in vitro evidence of modulated electro-hyperthermia treatment performance in combination with megavoltage radiation by clonogenic assay. Scientific Reports. 2018;8(1):16608.

83. Mijatovic T, Van Quaquebeke E, Delest B, Debeir O, Darro F, Kiss R. Cardiotonic steroids on the road to anti-cancer therapy. Biochimica et Biophysica Acta (BBA)-Reviews on Cancer. 2007;1776(1):32-57.

84. Minnaar C, Szasz A, Arrojo E, Lee S, Giorentini G, Borbenyi E. Summary and Update of the Method Modulated Electro-Hyperthermia. Oncothermia Journal, Special Edition. 2020:49-130.

85. Minnaar C, Szigeti G, Szasz A, Kotzen J. Review on the Use of Modulated Electro-Hyperthermia as a Stand-Alone Therapy in a Palliative Setting: Potential for Further Research? Journal of Cancer Therapy. 2022;13(6):362-77.

86. Minnaar CA, Kotzen JA, Ayeni OA, Naidoo T, Tunmer M, Sharma V, Vangu MD, Baeyens A. The effect of modulated electro-hyperthermia on local disease control in HIV-positive and -negative cervical cancer women in South Africa: Early results from a phase III randomised controlled trial. PLoS One. 2019;14(6):e0217894.

87. Minnaar CA, Kotzen JA, Ayeni OA, Vangu M-D-T, Baeyens A. Potentiation of the abscopal effect by modulated electro-hyperthermia in locally advanced cervical cancer patients. Frontiers in Oncology. 2020;10:376.

88. Minnaar CA, Maposa I, Kotzen JA, Baeyens A. Effects of modulated electro-hyperthermia (mEHT) on two and three year survival of locally advanced cervical cancer patients. Cancers. 2022;14(3):656.

89. Mishra M, Singh N, Ghatage P. Past, Present, and Future of Hyperthermic Intraperitoneal Chemotherapy (HIPEC) in Ovarian Cancer. Cureus. 2021;13(6):e15563.

90. Moon EJ, Sonveaux P, Porporato PE, Danhier P, Gallez B, Batinic-Haberle I, Nien Y-C, Schroeder T, Dewhirst MW. NADPH oxidase-mediated reactive oxygen species production activates hypoxia-inducible factor-1 (HIF-1) via the ERK pathway after hyperthermia treatment. Proceedings of the National Academy of Sciences. 2010;107(47):20477-82.

91. Nagata T, Kanamori M, Sekine S, Arai M, Moriyama M, Fujii T. Clinical study of modulated electro-hyperthermia for advanced metastatic breast cancer. Molecular and Clinical Oncology. 2021;14(5):1-7.

92. Nagy G, Meggyeshazi N, Szasz O, editors. Deep temperature measurements in oncothermia processes. Conference Papers in Science; 2013: Hindawi.

93. Oei AL, Kok HP, Oei SB, Horsman MR, Stalpers LJA, Franken NAP, Crezee J. Molecular and biological rationale of hyperthermia as radio- and chemosensitizer. Advanced Drug Delivery Reviews. 2020;163-164:84-97.

94. Ozel I, Duerig I, Domnich M, Lang S, Pylaeva E, Jablonska J. The Good, the Bad, and the Ugly: Neutrophils, Angiogenesis, and Cancer. Cancers. 2022;14(3):536.

95. Pang CLK, Zhang X, Wang Z, Ou J, Lu Y, Chen P, Zhao C, Wang X, Zhang H, Roussakow SV. Local modulated electro-hyperthermia in combination with traditional Chinese medicine vs. intraperitoneal chemoinfusion for the treatment of peritoneal carcinomatosis with malignant ascites: A phase II randomized trial. Mol Clin Oncol. 2017;6(5):723-32.

96. Papp E, Vancsik T, Kiss E, Szasz O. Energy absorption by the membrane rafts in the modulated electro-hyperthermia (mEHT). Open Journal of Biophysics. 2017;7(4):216-29.

97. Park MK, Lee CH, Lee H. Mouse models of breast cancer in preclinical research. Lab Anim Res. 2018;34(4):160-5.

98. Perou CM, Sørlie T, Eisen MB, van de Rijn M, Jeffrey SS, Rees CA, Pollack JR, Ross DT, Johnsen H, Akslen LA, Fluge O, Pergamenschikov A, Williams C, Zhu SX, Lønning PE, Børresen-Dale AL, Brown PO, Botstein D. Molecular portraits of human breast tumours. Nature. 2000;406(6797):747-52.

99. Petenyi FG, Garay T, Muhl D, Izso B, Karaszi A, Borbenyi E, Herold M, Herold Z, Szasz AM, Dank M. Modulated Electro-Hyperthermic (mEHT) Treatment in the Therapy of Inoperable Pancreatic Cancer Patients—A Single-Center Case-Control Study. Diseases. 2021;9(4):81.

100. Prasad B, Kim S, Cho W, Kim S, Kim JK. Effect of tumor properties on energy absorption, temperature mapping, and thermal dose in 13.56-MHz radiofrequency hyperthermia. Journal of thermal biology. 2018;74:281-9.

101. Pulaski BA, Ostrand-Rosenberg S. Mouse 4T1 Breast Tumor Model. Current Protocols in Immunology. 2000;39(1):20.2.1-.2.16.

102. Qin W, Akutsu Y, Andocs G, Suganami A, Hu X, Yusup G, Komatsu-Akimoto A, Hoshino I, Hanari N, Mori M. Modulated electro-hyperthermia enhances dendritic cell therapy through an abscopal effect in mice. Oncology Reports. 2014;32(6):2373-9.

103. Reddy D, Kumavath R, Barh D, Azevedo V, Ghosh P. Anticancer and antiviral properties of cardiac glycosides: a review to explore the mechanism of actions. Molecules. 2020;25(16):3596.

104. Ribatti D, Annese T, Ruggieri S, Tamma R, Crivellato E. Limitations of anti-angiogenic treatment of tumors. Translational Oncology. 2019;12(7):981-6.

105. Ribatti D, Pezzella F. Overview on the Different Patterns of Tumor Vascularization. Cells. 2021;10(3):639.

106. Riggio AI, Varley KE, Welm AL. The lingering mysteries of metastatic recurrence in breast cancer. British journal of cancer. 2021;124(1):13-26.

107. Roti JLR, Kampinga HH, Malyapa RS, Wright WD, Xu M. Nuclear matrix as a target for hyperthermic killing of cancer cells. Cell stress & chaperones. 1998;3(4):245-55.

108. Roussakow S, editor The history of hyperthermia rise and decline. Conference Papers in Science; 2013: Hindawi.

109. Sarkar FH, Adsule S, Li Y, Padhye S. Back to the future: COX-2 inhibitors for chemoprevention and cancer therapy. Mini Rev Med Chem. 2007;7(6):599-608.

110. Schettini F, Brasó-Maristany F, Kuderer NM, Prat A. A perspective on the development and lack of interchangeability of the breast cancer intrinsic subtypes. npj Breast Cancer. 2022;8(1):85.

111. Schito L. Hypoxia-Dependent Angiogenesis and Lymphangiogenesis in Cancer. In: Gilkes DM, editor. Hypoxia and Cancer Metastasis. Cham: Springer International Publishing; 2019. p. 71-85.

112. Schito L, Rey S. Hypoxia orchestrates the lymphovascular–immune ensemble in cancer. Trends in Cancer. 2022;8(9):771-84.

113. Schmid P, Rugo HS, Adams S, Schneeweiss A, Barrios CH, Iwata H, Diéras V, Henschel V, Molinero L, Chui SY. Atezolizumab plus nab-paclitaxel as first-line treatment for unresectable, locally advanced or metastatic triple-negative breast cancer (IMpassion130): updated efficacy results from a randomised, double-blind, placebo-controlled, phase 3 trial. The Lancet Oncology. 2020;21(1):44-59.

114. Schvarcz CA, Danics L, Krenács T, Viana P, Béres R, Vancsik T, Nagy Á, Gyenesei A, Kun J, Fonović M, Vidmar R, Benyó Z, Kaucsár T, Hamar P. Modulated Electro-Hyperthermia Induces a Prominent Local Stress Response and Growth Inhibition in Mouse Breast Cancer Isografts. Cancers (Basel). 2021;13(7).

115. Seynhaeve ALB, Amin M, Haemmerich D, van Rhoon GC, ten Hagen TLM. Hyperthermia and smart drug delivery systems for solid tumor therapy. Advanced Drug Delivery Reviews. 2020;163-164:125-44.

116. Shah SP, Roth A, Goya R, Oloumi A, Ha G, Zhao Y, Turashvili G, Ding J, Tse K, Haffari G. The clonal and mutational evolution spectrum of primary triple-negative breast cancers. Nature. 2012;486(7403):395-9.

117. Shevtsov M, Huile G, Multhoff G. Membrane heat shock protein 70: a theranostic target for cancer therapy. Philosophical Transactions of the Royal Society B: Biological Sciences. 2018;373(1738):20160526.

118. Siemann DW. The unique characteristics of tumor vasculature and preclinical evidence for its selective disruption by tumor-vascular disrupting agents. Cancer treatment reviews. 2011;37(1):63-74.

119. Song Y, Lee S-Y, Kim S, Choi I, Kim S-H, Shum D, Heo J, Kim A-R, Kim KM, Seo HR. Inhibitors of Na+/K+ ATPase exhibit antitumor effects on multicellular tumor spheroids of hepatocellular carcinoma. Scientific Reports. 2020;10(1):1-16.

120. Sung H, Ferlay J, Siegel RL, Laversanne M, Soerjomataram I, Jemal A, Bray F. Global cancer statistics 2020: GLOBOCAN estimates of incidence and mortality worldwide for 36 cancers in 185 countries. CA: a cancer journal for clinicians. 2021;71(3):209-49.

121. Suresh R, Diaz RJ. The remodelling of actin composition as a hallmark of cancer. Translational Oncology. 2021;14(6):101051.

122. Svensson A, Azarbayjani F, Bäckman U, Matsumoto T, Christofferson R. Digoxin inhibits neuroblastoma tumor growth in mice. Anticancer research. 2005;25(1A):207-12.

123. Szasz A. Heterogeneous Heat Absorption Is Complementary to Radiotherapy. Cancers. 2022;14(4):901.

124. Szasz A, Szasz N, Szasz O. Oncothermia: principles and practices: Springer Science & Business Media; 2010.

125. Szasz A, Szasz N, Szasz O, Szasz A, Szasz N, Szasz O. Oncothermia–A New Kind of Oncologic Hyperthermia. Oncothermia: Principles and Practices. 2011:173-392.

126. Szasz AM, Arrojo Alvarez EE, Fiorentini G, Herold M, Herold Z, Sarti D, Dank M. Meta-Analysis of Modulated Electro-Hyperthermia and Tumor Treating Fields in the Treatment of Glioblastomas. Cancers. 2023;15(3):880.

127. Szasz AM, Minnaar CA, Szentmártoni G, Szigeti GP, Dank M. Review of the clinical evidences of modulated electro-hyperthermia (mEHT) method: an update for the practicing oncologist. Frontiers in Oncology. 2019;9:1012.

128. Szász AM, Szász A, Szigeti G. The Immunogenic Connection of Thermal and Nonthermal Molecular Effects in Modulated Electro-Hyperthermia. Open Journal of Biophysics. 2023;13(4):103-42.

129. Szasz O. Bioelectromagnetic Paradigm of Cancer Treatment¡ªModulated Electro-Hyperthermia (mEHT). Open Journal of Biophysics. 2019;Vol.09No.02:12.

130. Szasz O, Szasz A. Heating, efficacy and dose of local hyperthermia. Open Journal of Biophysics. 2016;6(1):10-8.

131. Szigeti G, Szasz O, Hegyi G. Connections between Warburg's and Szentgyorgyi's Approach about the Causes of Cancer. Journal of Neoplasm. 2017;1(2-8):1-13.

132. Taleb M, Mohammadkhani N, Bahreini F, Ovais M, Nie G. Modulation of Tumor Vasculature Network: Key Strategies. Small Structures. 2022:2100164.

133. Thiruchenthooran V, Sánchez-López E, Gliszczyńska A. Perspectives of the application of non-steroidal anti-inflammatory drugs in cancer therapy: Attempts to overcome their unfavorable side effects. Cancers. 2023;15(2):475.

134. Thrall DE, LaRue SM, Pruitt AF, Case B, Dewhirst MW. Changes in tumour oxygenation during fractionated hyperthermia and radiation therapy in spontaneous canine sarcomas. International Journal of Hyperthermia. 2006;22(5):365-73.

135. Thrall DE, LaRue SM, Yu D, Samulski T, Sanders L, Case B, Rosner G, Azuma C, Poulson J, Pruitt AF. Thermal dose is related to duration of local control in canine sarcomas treated with thermoradiotherapy. Clinical Cancer Research. 2005;11(14):5206-14.

136. Thun MJ, Jacobs EJ, Patrono C. The role of aspirin in cancer prevention. Nature reviews Clinical oncology. 2012;9(5):259-67.

137. Torres A, Vivanco S, Lavín F, Pereda C, Chernobrovkin A, Gleisner A, Alcota M, Larrondo M, López MN, Salazar-Onfray F, Zubarev RA, González FE. Haptoglobin Induces a Specific Proteomic Profile and a Mature-Associated Phenotype on Primary Human Monocyte-Derived Dendritic Cells. International Journal of Molecular Sciences. 2022;23(13):6882.

138. Trenti A, Zulato E, Pasqualini L, Indraccolo S, Bolego C, Trevisi L. Therapeutic concentrations of digitoxin inhibit endothelial focal adhesion kinase and angiogenesis induced by different growth factors. Br J Pharmacol. 2017;174(18):3094-106.

139. Turabi KS, Deshmukh A, Paul S, Swami D, Siddiqui S, Kumar U, Naikar S, Devarajan S, Basu S, Paul MK. Drug repurposing—an emerging strategy in cancer therapeutics. Naunyn-Schmiedeberg's Archives of Pharmacology. 2022;395(10):1139-58.

140. Tveitarås MK, Selheim F, Sortland K, Reed RK, Stuhr L. Protein expression profiling of plasma and lungs at different stages of metastatic development in a human triple negative breast cancer xenograft model. PLOS ONE. 2019;14(5):e0215909.

141. van der Heijden AG, Dewhirst MW. Effects of hyperthermia in neutralising mechanisms of drug resistance in non-muscle-invasive bladder cancer. International journal of hyperthermia. 2016;32(4):434-45.

142. Vancsik T, Forika G, Balogh A, Kiss E, Krenacs T. Modulated electro-hyperthermia induced p53 driven apoptosis and cell cycle arrest additively support doxorubicin chemotherapy of colorectal cancer in vitro. Cancer medicine. 2019;8(9):4292-303.

143. Vancsik T, Kovago C, Kiss E, Papp E, Forika G, Benyo Z, Meggyeshazi N, Krenacs T. Modulated electro-hyperthermia induced loco-regional and systemic tumor destruction in colorectal cancer allografts. Journal of Cancer. 2018;9(1):41.

144. Vancsik T, Máthé D, Horváth I, Várallyaly AA, Benedek A, Bergmann R, Krenács T, Benyó Z, Balogh A. Modulated electro-hyperthermia facilitates NK-cell infiltration and growth arrest of human A2058 melanoma in a Xenograft model. Frontiers in Oncology. 2021;11:590764.

145. Vaupel PW, Kelleher DK. Pathophysiological and vascular characteristics of tumours and their importance for hyperthermia: Heterogeneity is the key issue. International Journal of Hyperthermia. 2010;26(3):211-23.

146. Veyssière H, Bidet Y, Penault-Llorca F, Radosevic-Robin N, Durando X. Circulating proteins as predictive and prognostic biomarkers in breast cancer. Clinical Proteomics. 2022;19(1):25.

147. Viana P, Hamar P. Targeting the heat shock response induced by modulated electro-hyperthermia (mEHT) in cancer. Biochimica et Biophysica Acta (BBA)-Reviews on Cancer. 2024:189069.

148. Vincze G, Szasz O, Szasz A. Generalization of the thermal dose of hyperthermia in oncology. Open Journal of Biophysics. 2015;5(04):97.

149. Vujaskovic Z, Poulson JM, Gaskin AA, Thrall DE, Page RL, Charles HC, MacFall JR, Brizel DM, Meyer RE, Prescott DM, Samulski TV, Dewhirst MW. Temperature-dependent changes in physiologic parameters of spontaneous canine soft tissue sarcomas after combined radiotherapy and hyperthermia treatment. International Journal of Radiation Oncology*Biology*Physics. 2000;46(1):179-85.

150. Vujaskovic Z, Song C. Physiological mechanisms underlying heat-induced radiosensitization. International Journal of Hyperthermia. 2004;20(2):163-74.

151. Wang J, Sun D, Huang L, Wang S, Jin Y. Targeting reactive oxygen species capacity of tumor cells with repurposed drug as an anticancer therapy. Oxidative medicine and cellular longevity. 2021;2021.

152. Wang X, Wang S-S, Huang H, Cai L, Zhao L, Peng R-J, Lin Y, Tang J, Zeng J, Zhang L-H. Effect of capecitabine maintenance therapy using lower dosage and higher frequency vs observation on disease-free survival among patients with early-stage triple-negative breast cancer who had received standard treatment: the SYSUCC-001 randomized clinical trial. Jama. 2021;325(1):50-8.

153. Wang Y, Ma Q, Zhang S, Liu H, Zhao B, Du B, Wang W, Lin P, Zhang Z, Zhong Y. Digoxin enhances the anticancer effect on non-small cell lung cancer while reducing the cardiotoxicity of adriamycin. Frontiers in pharmacology. 2020;11:186.

154. Westra A, Dewey W. Variation in sensitivity to heat shock during the cell-cycle of Chinese hamster cells in vitro. International Journal of Radiation Biology and Related Studies in Physics, Chemistry and Medicine. 1971;19(5):467-77.

155. Wismeth C, Dudel C, Pascher C, Ramm P, Pietsch T, Hirschmann B, Reinert C, Proescholdt M, Rümmele P, Schuierer G. Transcranial electro-hyperthermia combined with alkylating chemotherapy in patients with relapsed high-grade gliomas: phase I clinical results. Journal of neuro-oncology. 2010;98:395-405.

156. Wust P, Kortüm B, Strauss U, Nadobny J, Zschaeck S, Beck M, Stein U, Ghadjar P. Non-thermal effects of radiofrequency electromagnetic fields. Scientific Reports. 2020;10(1):13488.

157. Xia Y, Sun M, Huang H, Jin W-L. Drug repurposing for cancer therapy. Signal Transduction and Targeted Therapy. 2024;9(1):92.

158. Yang K-L, Huang C-C, Chi M-S, Chiang H-C, Wang Y-S, Hsia C-C, Andocs G, Wang H-E, Chi K-H. In vitro comparison of conventional hyperthermia and modulated electro-hyperthermia. Oncotarget. 2016;7(51):84082.

159. Yang KL, Huang CC, Chi MS, Chiang HC, Wang YS, Hsia CC, Andocs G, Wang HE, Chi KH. In vitro comparison of conventional hyperthermia and modulated electro-hyperthermia. Oncotarget. 2016;7(51):84082-92.

160. Yang T, Xiao H, Liu X, Wang Z, Zhang Q, Wei N, Guo X. Vascular normalization: a new window opened for cancer therapies. Frontiers in Oncology. 2021;11:719836.

161. Yin L, Duan J-J, Bian X-W, Yu S-c. Triple-negative breast cancer molecular subtyping and treatment progress. Breast Cancer Research. 2020;22(1):61.

162. Yoo HJ, Lim MC, Seo S-S, Kang S, Joo J, Park S-Y. Phase I/II clinical trial of modulated electro-hyperthermia treatment in patients with relapsed, refractory or progressive heavily treated ovarian cancer. Japanese Journal of Clinical Oncology. 2019;49(9):832-8.

163. Zagami P, Carey LA. Triple negative breast cancer: Pitfalls and progress. npj Breast Cancer. 2022;8(1):95.

164. Zager RA, Vijayan A, Johnson AC. Proximal tubule haptoglobin gene activation is an integral component of the acute kidney injury "stress response". Am J Physiol Renal Physiol. 2012;303(1):F139-48.

165. Zelenay S, Van Der Veen AG, Böttcher JP, Snelgrove KJ, Rogers N, Acton SE, Chakravarty P, Girotti MR, Marais R, Quezada SA. Cyclooxygenase-dependent tumor growth through evasion of immunity. Cell. 2015;162(6):1257-70.

166. Zhang H, Qian DZ, Tan YS, Lee K, Gao P, Ren YR, Rey S, Hammers H, Chang D, Pili R. Digoxin and other cardiac glycosides inhibit HIF-1α synthesis and block tumor growth. Proceedings of the National Academy of Sciences. 2008;105(50):19579-86.

167. Zhang Q, Zhu B, Li Y. Resolution of Cancer-Promoting Inflammation: A New Approach for Anticancer Therapy. Front Immunol. 2017;8:71.

168. Zhang Z, Wang Y, Ma Q, Zhang S, Liu H, Zhao B, Liu R, Wang W, Du B, Zhong Y, Kong D. Biomimetic carrier-free nanoparticle delivers digoxin and doxorubicin to exhibit synergetic antitumor activity in vitro and in vivo. Chemical Engineering Journal. 2021;406:126801.

169. Zhou W, Yang L, Nie L, Lin H. Unraveling the molecular mechanisms between inflammation and tumor angiogenesis. Am J Cancer Res. 2021;11(2):301-17.

170. Zhou Y, Zhou Y, Yang M, Wang K, Liu Y, Zhang M, Yang Y, Jin C, Wang R, Hu R. Digoxin sensitizes gemcitabine-resistant pancreatic cancer cells to gemcitabine via inhibiting Nrf2 signaling pathway. Redox biology. 2019;22:101131.

9. Bibliography of Candidate's publications

Publications related to the dissertation

Bokhari, S. M. Z., Aloss, K., Leroy Viana, P. H., Schvarcz, C. A., Besztercei, B., Giunashvili, N., Bócsi, D., Koós, Z., Balogh, A., & Benyó, Z. (2024). Digoxin-Mediated Inhibition of Potential Hypoxia-Related Angiogenic Repair in Modulated Electro-Hyperthermia (mEHT)-Treated Murine Triple-Negative Breast Cancer Model. *ACS Pharmacology & Translational Science, 7*(2), 456-466. (IF=6.0)

Bokhari, S. M. Z., & Hamar, P. (2023). Vascular Endothelial Growth Factor-D (VEGF-D): An Angiogenesis Bypass in Malignant Tumors. *International Journal of Molecular Sciences, 24*(17), 13317. (IF=5.6)

Giunashvili, N., Thomas, J. M., Schvarcz, C. A., Viana, P. H. L., Aloss, K., **Bokhari, S. M. Z.**, Koós, Z., Bócsi, D., Major, E., & Balogh, A. (2024). Enhancing therapeutic efficacy in triple-negative breast cancer and melanoma: synergistic effects of modulated electro-hyperthermia (mEHT) with NSAIDs especially COX-2 inhibition in in vivo models. *Molecular Oncology*. (IF= 6.6)

Publications not related to the dissertation

Aloss, K., **Bokhari, S. M. Z.**, Leroy Viana, P. H., Giunashvili, N., Schvarcz, C. A., Szénási, G., Bócsi, D., Koós, Z., Storm, G., Miklós, Z., Benyó, Z., & Hamar, P. (2024). Modulated Electro-Hyperthermia Accelerates Tumor Delivery and Improves Anticancer Activity of Doxorubicin Encapsulated in Lyso-Thermosensitive Liposomes in 4T1-Tumor-Bearing Mice. *International Journal of Molecular Sciences, 25*(6), 3101. (IF=5.6)

Dora, D., **Bokhari, S. M. Z.**, Aloss, K., Takacs, P., Desnoix, J. Z., Szklenárik, G., Hurley, P. D., & Lohinai, Z. (2023). Implication of the Gut Microbiome and Microbial-Derived Metabolites in Immune-Related Adverse Events: Emergence of Novel Biomarkers for Cancer Immunotherapy. *International Journal of Molecular Sciences, 24*(3), 2769. (IF=5.6)

Viana PH, Schvarcz CA, Danics LO, Besztercei B, Aloss K, **Bokhari SM**, Giunashvili N, Bócsi D, Koós Z, Benyó Z, Hamar P. Heat shock factor 1 inhibition enhances the

effects of modulated electro hyperthermia in a triple negative breast cancer mouse model. Scientific Reports. 2024 Apr 8;14(1):8241. (IF=4.6)

10. Acknowledgments

I would like to thank my supervisor, Professor Péter Hamar, for his guidance and encouragement during the four years of my PhD studies. I am grateful for his professional advice and continuous support for my personal and professional growth.

I am thankful to Professor Zoltán Benyó for providing the place and infrastructure for my research at the Institute of Translational Medicine and for his professional advice and support during my PhD studies.

I am also extremely grateful to my colleagues Pedro Viana, Kenan Aloss and Nino Guinashville for their endless support and friendship. I would like to thank my senior colleague Csaba Schvarcz for patiently teaching me in-vivo techniques and for his continuous support. I would also like to express my sincere gratitude to all my co-authors for their efforts and to all former and current colleagues at the Institute of Translational Medicine for their support.

I am truly thankful to Dr. Forika Gertrud for reviewing my thesis; her professional remarks, suggestions, and corrections contributed greatly to the improvement of my work.

I am thankful to my parents and my brother Asad for always believing in me and listening to all my rants over failed experiments. Finally, I am immensely thankful and grateful to my loving husband Hassan who made my dreams his own and moved to another side of the world for me and my PhD dream.

This PhD would not have been possible without the kind support of these amazing people, and I am forever thankful to all of them.